Heterogeneous reaction of $ClONO_2$ with TiO_2 and SiO_2 aerosol particles: implications for stratospheric particle injection for climate engineering

M. J. Tang[1,2,7], J. Keeble[1], P. J. Telford[1,3], F. D. Pope[4], P. Braesicke[5], P. T. Griffiths[1,3], N. L. Abraham[1,3], J. McGregor[6], I. M. Watson[2], R. A. Cox[1], J. A. Pyle[1,3], M. Kalberer[1,*]

1 Department of Chemistry, University of Cambridge, Cambridge CB2 1EW, UK

2 School of Earth Sciences, University of Bristol, Bristol BS8 1RJ, UK

3 National Centre for Atmospheric Science, NCAS, UK

4 School of Geography, Earth and Environmental Sciences, University of Birmingham, Birmingham B15 2TT, UK

5 IMK-ASF, Karlsruhe Institute of Technology, Karlsruhe, Germany

6 Department of Chemical and Biological Engineering, University of Sheffield, Sheffield S1 3JD, UK

7 State Key Laboratory of Organic Geochemistry, Guangzhou Institute of Geochemistry, Chinese Academy of Sciences, Guangzhou 510640, China

Correspondence: M. Kalberer (markus.kalberer@atm.ch.cam.ac.uk)

Abstract

Deliberate injection of aerosol particles into the stratosphere is a potential climate engineering scheme. Particles injected into the stratosphere would scatter solar radiation back to space, thereby reducing the temperature at the Earth's surface and hence the impacts of global warming. Minerals such as TiO_2 or SiO_2 are among the potentially suitable aerosol materials for stratospheric particle injection due to their greater light scattering ability compared to stratospheric sulfuric acid particles. However, the heterogeneous reactivity of mineral particles towards trace gases important for stratospheric chemistry largely remains unknown, precluding reliable assessment of their impacts on stratospheric ozone which is of key environmental significance. In this work we have investigated for the first time the heterogeneous hydrolysis of $ClONO_2$ on TiO_2 and SiO_2 aerosol particles at room temperature and at different relative humidities (RH), using an aerosol flow tube. The uptake coefficient, $\gamma(ClONO_2)$, on TiO_2 was ~1.2×10^{-3} at 7% and remaining unchanged at 33% RH, and increased for SiO_2 from ~2×10^{-4} at 7% RH to ~5×10^{-4} at 35% RH, reaching a value of ~6×10^{-4} at 59% RH. We have also examined the impacts of a hypothetical TiO_2 injection on stratospheric chemistry using the UKCA chemistry-climate model in which heterogeneous hydrolysis of N_2O_5 and $ClONO_2$ on TiO_2 particles is considered. A TiO_2 injection scenario with a solar radiation scattering effect very similar to the eruption of Mt. Pinatubo was constructed. It is found that compared to the eruption of Mt. Pinatubo, TiO_2 injection causes less ClOx activation and less ozone destruction in the lowermost stratosphere, while reduced depletion of N_2O_5 and NOx in the middle stratosphere results in decreased ozone levels. Overall, no significant difference in the vertically integrated ozone abundancies is found between TiO_2 injection and the eruption of Mt. Pinatubo. Future work required to further assess the impacts of TiO_2 injection on stratospheric chemistry is also discussed.

1 Introduction

Climate engineering (also known as geoengineering), the deliberate and large-scale intervention in the Earth's climatic system to reduce global warming (Shepherd, 2009), has been actively discussed by research communities and is also beginning to surface in the public consciousness. The injection of aerosol particles (or their precursors) into the stratosphere to scatter solar radiation back into space is one of the solar-radiation management (SRM) schemes proposed for climate engineering (Crutzen, 2006). Sulfuric acid particles, due to their natural presence in the stratosphere (SPARC, 2006), have been the main focus of stratospheric particle injection research (Crutzen, 2006; Ferraro et al., 2011; Kravitz et al., 2013; Tilmes et al., 2015; Jones et al., 2016). Very recently, minerals with refractive indices higher than sulphuric acid, e.g., TiO_2 and SiO_2, have been proposed as possible alternative particles to be injected into the stratosphere for climate engineering (Pope et al., 2012). For example, the refractive index at 550 nm is 2.5 for TiO_2 and 1.5 for stratospheric sulfuric acid particles. If the size of TiO_2 particles used for SRM can be optimized, it is estimated that compared to sulfuric acid particles, the use of TiO_2 requires a factor of ~3 less in mass (and a factor of ~7 less in volume) in order to achieve the same solar radiation scattering effect (Pope et al., 2012).

Injecting particles into the stratosphere would increase the amount of aerosol particles in the stratosphere, thus increasing the surface area available for heterogeneous reactions (e.g., R1a, R1b, and R1c), whose effects on stratospheric chemistry and in particular on stratospheric ozone depletion have been well documented for sulfuric acid particles (Molina et al., 1996; Solomon, 1999). The background burden of sulfuric acid particles in the stratosphere, i.e. during periods with low volcanic activities, is 0.65±0.2 Tg (SPARC, 2006). The eruption of Mt. Pinatubo in 1991 delivered an additional ~30 Tg sulfuric acid particles into the stratosphere (Guo et al., 2004) and subsequently produced record low levels of stratospheric ozone

(McCormick et al., 1995), in addition to causing substantial surface cooling (Dutton and Christy, 1992). Observation and modelling studies have further suggested that, after the eruption of Mt. Pinatubo, significant change in the partitioning of nitrogen and chlorine species in the stratosphere occurred (Fahey et al., 1993; Wilson et al., 1993; Solomon, 1999), caused by heterogeneous reactions of N_2O_5 and $ClONO_2$ (R1a-R1c):

$N_2O_5 + H_2O + surface \rightarrow HNO_3 + HNO_3$ (R1a)

$ClONO_2 + H_2O + surface \rightarrow HNO_3 + HOCl$ (R1b)

$ClONO_2 + HCl + surface \rightarrow HNO_3 + Cl_2$ (R1c)

Therefore, before any types of material can be considered for stratospheric particle injection, their impact on stratospheric chemistry and ozone in particular has to be well understood (Tilmes et al., 2008; Pope et al., 2012).

Heterogeneous reactions on sulfuric acid and polar stratospheric clouds (PSCs) have been extensively studied and well characterized (Crowley et al., 2010; Ammann et al., 2013; Burkholder et al., 2015). However, the reactivity of minerals (e.g., TiO_2 and SiO_2) towards reactive trace gases in the stratosphere has received much less attention. For example, the heterogeneous reactions of $ClONO_2$ with silica (SiO_2) and alumina (Al_2O_3) in the presence of HCl (R1c) have only been explored by one previous study (Molina et al., 1997) in which minerals coated on the inner wall of a flow tube were used. Further discussion of this work is provided in Section 4.4. The lack of high quality kinetic data for important reactions impedes reliable assessment of assessing the impact of injecting mineral particles into the stratosphere on stratospheric ozone (Pope et al., 2012). TiO_2 is an active photo-catalyst (Shang et al., 2010; Chen et al., 2012; Romanias et al., 2012; Kebede et al., 2013; George et al., 2015) and the effects of its photochemical reactions on stratospheric chemistry, if injected into stratosphere

for the purpose of climate engineering, have never been assessed. Therefore, its atmospheric heterogeneous photochemistry deserves further investigation.

To address these issues, in our previous work we have investigated the heterogeneous reactions of N_2O_5 with TiO_2 (Tang et al., 2014c) and SiO_2 (Tang et al., 2014a) particles (R1a). That work is extended here to the investigation of the heterogeneous hydrolysis of $ClONO_2$ on TiO_2 and SiO_2 (R1b) using an aerosol flow tube. There are only a few previous studies in which the reactions of $ClONO_2$ with airborne particles or droplets have been examined. For example, the interaction of $ClONO_2$ with sulfuric acid aerosol particles was investigated using aerosol flow tubes (Hanson and Lovejoy, 1995; Ball et al., 1998; Hanson, 1998). Droplet train techniques were used to study the heterogeneous reactions of $ClONO_2$ with aqueous droplets containing sulfuric acid (Robinson et al., 1997) or halide (Deiber et al., 2004). The interaction of $ClONO_2$ with airborne water ice particles was also examined (Lee et al., 1999). Our experimental work, carried out at room temperature and at different RH, is the first study which has investigated the heterogeneous interaction of $ClONO_2$ with airborne mineral particles. In the lower stratosphere into which particles would be injected, typical temperature and RH ranges are 200-220 K and <40%, respectively (Dee et al., 2011). We note that while our experimental work covers the RH range relevant for the lower stratosphere, it has only been performed at room temperature instead of 200-220 K due to experimental challenges.

$ClONO_2$ may also play a role in tropospheric chemistry (Finlayson-Pitts et al., 1989) though its presence in the troposphere has not yet been confirmed by field measurements. The importance of Cl atoms in tropospheric oxidation capacity has received increasing attention in recent years (Simpson et al., 2015), and precursors of Cl atoms, e.g., $ClNO_2$ (Osthoff et al., 2008; Thornton et al., 2010; Phillips et al., 2012; Bannan et al., 2015; Wang et al., 2016), Cl_2 (Spicer et al., 1998; Riedel et al., 2012; Liao et al., 2014), and HOCl (Lawler et al., 2011), have been detected in the troposphere at various locations. Cl atoms react with O_3 to form ClO

radicals, which react with NO_2 to produce $ClONO_2$. The uptake of $ClONO_2$ by aerosol particles (R1b, R1c) may recycle $ClONO_2$ to more photolabile species (HOCl or Cl_2) and thus amplify the impact of Cl atoms on tropospheric oxidation capacity (Finlayson-Pitts et al., 1989; Deiber et al., 2004). Considering the widespread occurrence of reactive chlorine species (Simpson et al., 2015) and mineral dust particles (Textor et al., 2006; Ginoux et al., 2012; Tang et al., 2016) in the troposphere, our laboratory measurements can also have strong implications for tropospheric chemistry.

Using the UKCA (United Kingdom Chemistry and Aerosol model) chemistry-climate model, a preliminary assessment of the effect of injecting TiO_2 into the stratosphere on stratospheric chemistry and ozone was discussed in our previous work (Tang et al., 2014c). This model was also used to investigate stratospheric ozone change due to volcanic sulfuric acid particles after the eruption of Mt. Pinatubo in 1991 (Telford et al., 2009). In the previous work (Tang et al., 2014c), we used the UKCA model to construct a case study in which TiO_2 aerosols were distributed in the stratosphere in a similar way to the volcanic sulfuric acid particles after the eruption of Mt. Pinatubo so that the solar radiation scattering effect was similar for the two scenarios; however, the only heterogeneous reaction on TiO_2 particles considered was the uptake of N_2O_5 (R1a). Injection of solid aerosols into the stratosphere can have a significant impact on ozone mixing ratios when heterogeneous reactions involving chlorine are considered (Weisenstein et al., 2015). Several previous studies (Jackman et al., 1998; Danilin et al., 2001; Weisenstein et al., 2015) have considered the effects of solid alumina particles on stratospheric chemistry; however, there is only very limited assessment of other potential solid aerosol compositions (e.g., TiO_2 and diamond) (Tang et al., 2014c). Here we expand upon the previous literature by considering in our model a number of heterogeneous reactions with new kinetic data on TiO_2. In our current work the heterogeneous hydrolysis of $ClONO_2$ on TiO_2 particles (R1b) has been included, using our new experimental data. The

changes in stratospheric ozone and reactive nitrogen and chlorine species are assessed by comparing to the impact of the Mt. Pinatubo eruption.

2 Experimental section

The heterogeneous reaction of $ClONO_2$ with aerosol particles was investigated at different RH using an atmospheric pressure aerosol flow tube (AFT). In addition, its uptake onto Pyrex glass was also studied, using a coated wall flow tube. N_2 was used as carrier gas, and all the experiments were carried out at 296±2 K.

2.1 Aerosol flow tube

2.1.1 Flow tube

A detailed description of the AFT was given in our previous work (Tang et al., 2014a; Tang et al., 2014c), and only the key features are described here. The flow tube, as shown in Figure 1, is a horizontally-mounted Pyrex glass tube (i.d.: 3.0 cm; length: 100 cm). The total flow in the AFT was 1500 mL/min, leading to a linear flow velocity of 3.54 cm s^{-1} and a maximum residence time of ~30 s. The Reynolds number is calculated to be 69, suggesting a laminar flow condition in the flow tube. Under our experimental conditions, the entrance length needed to develop the laminar flow is ~12 cm. The mixing length is calculated to be ~14 cm, using a diffusion coefficient of 0.12 cm^2 s^{-1} for $ClONO_2$ in N_2 at 296 K (Tang et al., 2014b). Only the middle part of the flow tube (30-80 cm) was used to measure the uptake kinetics.

A commercial atomizer (Model 3076, TSI, USA) was used to generate an ensemble of mineral aerosols. N_2 at ~3 bar was applied to the atomizer to disperse the mineral/water mixture (with a TiO_2 or SiO_2 mass fraction of ~0.5%), resulting in an aerosol flow of 3000 mL/min. The aerosol flow was delivered through two diffusion dryers, and the resulting RH was adjusted by varying the amount of silica gel in the diffusion dryers. 1200 mL/min flow was pumped away through F1, and the remaining flow (1800 mL/min) was then delivered through a cyclone

(TSI, USA) to remove super-micrometre particles. This cyclone has a cut-off size of 800 nm at a flow rate of 1000 mL/min. The aerosol flow could be delivered through a filter to remove all the particles (to measure the wall loss rate), or alternatively the filter could be bypassed to introduce aerosol particles into the AFT (to measure the total loss rate). Beyond that point, 300 mL/min was sampled by a scanning mobility particle sizer (SMPS), and the remaining 1500 mL/min flow was delivered into the AFT via the side arm. Mineral aerosols were characterized online using a SMPS, consisting of a differential mobility analyser (DMA, TSI 3081) and a condensation particle counter (CPC, TSI 3775) which was operated with a sampling flow rate of 300 mL/min. The sheath flow of the DMA was set to 2000 mL/min, giving a detectable mobility size range of 19-882 nm. The time resolution of the SMPS measurement was 150 s.

The bottom 30 cm of the AFT was coaxially inserted into another Pyrex tube (inner diameter: 4.3 cm; length: 60 cm). A sheath flow (F2, 1500 mL/min) was delivered through the annular space between the two coaxial tubes. The sheath flow has the same linear velocity as the aerosol flow to minimize the turbulence at the end of the aerosol flow tube where the two flows joined. Gases could exchange between the sheath flow and the aerosol flow because of their large diffusion coefficients (~0.1 $cm^2 s^{-1}$) (Tang et al., 2014b), while aerosol particles remained in the centre due to their much smaller diffusion coefficients, i.e. 10^{-7}-10^{-6} $cm^2 s^{-1}$ (Hinds, 1996). At the end of the large Pyrex tube, a flow of 500 mL/min was sampled through a 1/4'' FEP tube which intruded 1-2 mm into the flow close to the wall of the Pyrex tube. This gas-particle separation method enabled particle-free gas to be sampled, despite very high aerosol concentrations used in the AFT. Sampling particle-free gas prevents particles from deposition onto the inner wall of the sampling tube, and therefore minimizes the undesired loss of the reactive trace gases (e.g., $ClONO_2$ in this study) during their transport to the detector. More detailed discussion of this gas-particle separation method used in the aerosol flow experiments are provided elsewhere (Rouviere et al., 2010; Tang et al., 2012).

2.1.2 $ClONO_2$ synthesis

$ClONO_2$ was synthesized in the lab by reacting Cl_2O with N_2O_5 (Davidson et al., 1987; Fernandez et al., 2005). N_2O_5 crystals were synthesized by trapping the product formed from mixing NO with O_3 in large excess (Fahey et al., 1985). The synthesis and purification is detailed in our previous study (Tang et al., 2014c). Cl_2O was synthesized by reacting HgO with Cl_2 (Renard and Bolker, 1976; Molina et al., 1977). Cl_2 from a lecture bottle was first trapped as yellow-green liquid (a few mL) in a glass vial at -76 ^oC using an ethanol-dry ice bath. It was then warmed up to room temperature so that all the Cl_2 was evaporated and transferred to the second glass vessel which contained HgO powders in excess and was kept at -76 ^oC. The glass vessel containing liquid Cl_2 and HgO powders was sealed and kept at -76 ^oC overnight. It was then warmed up to room temperature to evaporate and transfer the formed Cl_2O and any remaining Cl_2 to the third glass vial kept at -76 ^oC. Liquid Cl_2O appeared dark reddish-brown in colour.

The third vessel containing Cl_2O was warmed up to room temperature to evaporate and transfer Cl_2O to the fourth vial which contained synthesized N_2O_5 and was kept at -76 ^oC. The vial containing Cl_2O and N_2O_5 was sealed and kept at -50 ^oC for 2-3 days in a cryostat. In this work Cl_2O was in slight excess compared to N_2O_5, and thus all the white powder (solid N_2O_5) was consumed. $ClONO_2$ is liquid at -50 ^oC, with a colour similar to liquid Cl_2. The major impurity of our synthesized $ClONO_2$ was Cl_2O, and the boiling temperature at 760 Torr is 2 ^oC for Cl_2O and ~22 ^oC for $ClONO_2$ (Stull, 1947; Renard and Bolker, 1976). To purify our synthesized $ClONO_2$, the vial containing $ClONO_2$ was warmed up to 5 ^oC and connected to a small dry N_2 flow via a T-piece for a few hours. Note that the N_2 flow was not delivered into the vial but instead served as a dry atmosphere at ~760 Torr. Cl_2O was boiled at 5 ^oC and diffused passively into the N_2 flow. Cl_2 was also removed because its boiling temperature is -34 ^oC (Stull, 1947). The amount of N_2O_5 in $ClONO_2$ was minimized because Cl_2O was in excess.

In addition, the vapour pressure (a few mTorr) of N_2O_5 (Stull, 1947) is >100 times lower than that of $ClONO_2$ (~1 Torr) at around -76 ^oC (Schack and Lindahl, 1967; Ballard et al., 1988; Anderson and Fahey, 1990); therefore, even if N_2O_5 was present in the gas phase, its amount would be negligible compared to $ClONO_2$.

2.1.3 $ClONO_2$ detection

The $ClONO_2$ vial was stored at -76 ^oC in the dark using a cryostat. A small dry N_2 flow (a few mL/min, F3) was delivered into the vial to elute gaseous $ClONO_2$. The $ClONO_2$ flow was delivered through 1/8'' FEP tubing in a stainless-steel injector into the centre of the aerosol flow tube. The position of the injector could be adjusted to vary the interaction time of $ClONO_2$ with aerosols in the flow tube.

The flow sampled from the flow tube (500 mL/min) was mixed with ~5 mL/min NO (100 ppmv in N_2) and then delivered into a glass reactor heated to 130 ^oC. The initial NO mixing ratio (in the absence of $ClONO_2$) in the reactor was ~1000 ppbv (or ~1.8×10^{13} molecule cm^{-3}). The volume of the glass reactor (inner diameter: 2.0 cm; length: 10 cm) is ~30 cm^3, corresponding to an average residence time of ~2.6 s at 130 ^oC. The scheme used in our work to detect $ClONO_2$ is shown in Scheme 1 and explained in detail below. $ClONO_2$ was thermally decomposed in the reactor to ClO and NO_2 (R2, where M is the third molecule, e.g., N_2), and ClO was then titrated by NO in excess (R3):

$ClONO_2 + M \rightarrow ClO + NO_2 + M$ (R2)

$ClO + NO \rightarrow Cl + NO_2$ (R3)

Cl atoms produced in reaction (R3) further reacted with $ClONO_2$ (R4), and the NO_3 radicals formed were titrated by NO (R5):

$Cl + ClONO_2 \rightarrow Cl_2 + NO_3$ (R4)

$NO_3 + NO \rightarrow NO_2 + NO_2$ (R5)

If the thermal dissociation of $ClONO_2$ (R2) and the scavenging of ClO and NO_3 radicals by NO (R3, R4) all reach completion, the initial mixing ratio of $ClONO_2$ is equal to the decrease in the NO mixing ratios before and after introducing $ClONO_2$ into the reactor (Anderson and Fahey, 1990).

The lifetime of $ClONO_2$ with respect to thermal dissociation (R2) at 130 ^oC was estimated to be ~0.2 s at 160 Torr (Anderson and Fahey, 1990), and further increase in pressure to ~760 Torr would increase the decomposition rate and reduce its lifetime. The lifetime of $ClONO_2$ with respect to reaction (R4) is not critical for our purpose although it enhances the overall decay of $ClONO_2$ in the reactor. The second order rate constants are 1.3×10^{-11} cm^3 $molecule^{-1}$ s^{-1} for the reaction of ClO with NO and 2.3×10^{-11} cm^3 $molecule^{-1}$ s^{-1} for the reaction of NO_3 with NO at 130 ^oC (Burkholder et al., 2015), giving lifetimes of ~4×10^{-3} s for ClO with respect to reaction (R3) and ~2×10^{-3} s for NO_3 with respect to reaction (R5) in the presence of ~1000 ppbv NO in the reactor. To conclude, under our experimental conditions, the residence time of the gas flow in the heated reactor was long enough for the completion of thermal dissociation of $ClONO_2$ (R2) and titrations of ClO and NO_3 by NO (R3 and R5).

The flow exiting the reactor was sampled by a chemiluminescence-based NOx analyser (Model 200E, Teledyne Instruments, USA), which has a sampling flow rate of 500 mL/min (±10%). This instrument has two modes. In the first mode NO is measured by detecting the chemiluminescence of exited NO_2 (NO_2^*) produced by reacting NO with O_3 in excess. The gas flow can also be passed through a convertor cartridge filled with molybdenum (Mo) chips heated to 315 ^oC and all the NO_2 (and very likely also some of other NOy, e.g., HONO, HNO_3) is converted to NO; in this mode the total NO (initial NO and NO converted from NO_2 etc.) is measured and termed as NOx. The two modes are periodically switched, and the instrument has a detection limit of 0.5 ppbv with a time resolution of 1 min.

The response of measured NO and NOx mixing ratios to the introduction of $ClONO_2$ into the AFT is displayed in Figure 2. Both the sheath flow and the flow in the AFT were set to 1500 mL/min (dry N_2), and the injector was at 40 cm. The introduction of $ClONO_2$ into the AFT at ~20 min leads to the decrease of NO (solid curve in Figure 2a) from ~1100 ppbv to ~400 ppbv, and NO recovered to its initial level after stopping the $ClONO_2$ flow at ~120 min. The $ClONO_2$ mixing ratio (solid curve in Figure 2b), derived from the change in the NO mixing ratio, was very stable over 100 min. As expected, the introduction of $ClONO_2$ into the system led to the increase of the measured NOx mixing ratio (dashed curve in Figure 2a). Ideally the increase in NOx mixing ratios due to the introduction of $ClONO_2$ should be equal to the $ClONO_2$ mixing ratio. The nitrogen balance (dashed curve in Figure 2b), defined as the difference in the $ClONO_2$ mixing ratios (equal to the change in NO mixing ratios) and the change of the NOx mixing ratios, is essentially zero within the experimental noise level. This gives us further confidence in the purity of our synthesized $ClONO_2$: under our current detection scheme the change in the NOx mixing ratios will be twice of the N_2O_5 mixing ratio, and therefore N_2O_5 contained in the $ClONO_2$ flow as an impurity was negligible. This method provides a simple and relatively selective method to quantify $ClONO_2$, and could be used to calibrate other $ClONO_2$ detection methods (Anderson and Fahey, 1990). One previous study used a similar method to detect $ClONO_2$ in their experiments of $ClONO_2$ uptake onto sulfuric acid aerosol particles (Ball et al., 1998), with the only difference being that in their study NO was detected by its absorption at 1845.5135 cm^{-1}. Their reported $\gamma(ClONO_2)$ onto sulfuric acid aerosol particles are in good agreement with those measured by other studies in which $ClONO_2$ was measured using mass spectrometry. This suggests that the indirect detection method of $ClONO_2$ utilized by Ball et al. (1998) and in this work can be used to investigate the uptake of $ClONO_2$ onto aerosol particles.

2.2 Coated-wall flow tube

The coated-wall flow tube, a Pyrex glass tube with an inner diameter of 30 mm, was used to measure the uptake of $ClONO_2$ onto fresh Pyrex glass. The inner wall was rinsed with diluted NaOH solution and then by methanol and deionized water. A flow of 1500 mL/min, humidified to the desired RH, was delivered into the top of the flow tube via a side arm. A small N_2 flow was used to elute the liquid $ClONO_2$ sample, and the flow was then delivered through a 1/8'' Teflon tube in a stainless steel injector into the centre of the flow tube. The position of the injector could be changed to vary the interaction time between $ClONO_2$ and the inner wall of the flow tube. At the bottom of the flow tube, a flow of 500 mL/min was sampled through another side arm, mixed with ~5 mL/min NO (100 ppmv in N_2), and then delivered into a glass reactor heated to 130 ^oC. The flow exiting the heated glass reactor was then sampled into a NOx analyser. The method used to detect $ClONO_2$ is detailed in Section 2.1. The remaining flow (~1000 mL/min) went through a RH sensor into the exhaust.

The linear flow velocity in the flow tube is 3.54 cm s^{-1} with a Reynolds number of 69, suggesting that the flow is laminar. The length of the flow tube, defined as the distance between the side arm through which the main flow was delivered into the flow tube and the other side arm through which 500 mL/min was sampled from the flow tube into the NOx analyser, is 100 cm, giving a maximum residence time of ~30 s. The entrance length required to fully develop the laminar flow and the mixing length required to fully mix $ClONO_2$ with the main flow are both less than 15 cm. The loss of $ClONO_2$ onto the inner wall was measured using the middle part (30-80 cm) of the flow tube.

2.3 Chemicals

NO (>99% purity) in a lecture bottle and the 100 ppmv (±1 ppmv) NO in N_2 were supplied by CK Special Gas (UK). Pure Cl_2 (with a purity of >99.5%) in a lecture bottle and HgO

(yellow powder, with a purity of >99%) were provided by Sigma-Aldrich (UK). N_2 and O_2 were provided by BOC Industrial Gases (UK). P25 TiO_2, with an anatase to rutile ratio of 3:1, was supplied by Degussa-Hüls AG (Germany). SiO_2 powders with a stated average particle size (aggregate) of 200-300 nm were purchased from Sigma-Aldrich (UK). The BET surface area is 8.3 $m^2\ g^{-1}$ for TiO_2 (Tang et al., 2014c) and ~201 $m^2\ g^{-1}$ for SiO_2 (Tang et al., 2014a).

3 Model description

The UKCA chemistry-climate model in its coupled stratosphere-troposphere configuration, which combines both the tropospheric (O'Connor et al., 2014) and stratospheric (Morgenstern et al., 2009) schemes, was used to simulate the effect of heterogeneous hydrolysis of N_2O_5 (R1a) and $ClONO_2$ (R1b) on TiO_2. In this model the chemical cycles of Ox, HOx and NOx, the oxidation of CO, ethane, propane and isoprene, chlorine and bromine chemistry are all included. The model also includes a detailed treatment of polar processes. UKCA uses an equilibrium scheme to determine the presence and abundance of NAT and ice PSCs, assuming thermodynamic equilibrium with gas-phase HNO_3 and water vapor (Chipperfield, 1999). Chlorine activation through heterogeneous reactions occurs on both PSC particles and sulfuric acid aerosols (Morgenstern et al., 2009).

The same approach used to investigate the effects of the eruption of Mt. Pinatubo on stratospheric ozone (Telford et al., 2009) is adopted in this study. Using the UKCA model in a "nudged" configuration, Telford et al. (2009) evaluated the difference of stratospheric ozone with and without the additional sulfuric acid aerosols caused by the eruption of Mt. Pinatubo. "Nudging", or Newtonian relaxation, is a method that provides a realistic representation of short term dynamical features by adjusting modelled dynamical variables towards meteorological reanalysis data. This process was detailed by a previous study (Telford et al., 2008), and has been used in a number of other models (Jeuken et al., 1996; Takemura

et al., 2000; Hauglustaine et al., 2004; Schmidt et al., 2006). By constraining the dynamics of the model in this way the model is able to faithfully reproduce the meteorology of the time period around the eruption of Mt Pinatubo.

In our current study three simulations are used to assess the effects of TiO_2 particle injection into the stratosphere. All three simulations are started from a spun-up initial condition and run from December 1990 to January 1993. In the base scenario (S1), an aerosol climatology is used which represents the background loading of stratospheric sulphate aerosol. Alongside S1 two further simulations were performed, one representing the eruption of Mt. Pinatubo in June 1991 (S2) and a second (S3) in which the Mt. Pinatubo eruption is replaced with a single injection of TiO_2 particles on the same date. The simulations are set up so that the radiative impacts at the surface are comparable between S2 and S3. Pope et al. (2012) have proposed that 10 Tg of TiO_2 aerosol particles with an assumed radius of 70 nm are required in order to achieve the same solar radiation scattering effect as the eruption of Mt. Pinatubo. The total surface area of TiO_2 is calculated from the mass of TiO_2 particles, using a density of 4.23 g cm^{-3} and an assumed radius of 70 nm, and the global distribution of TiO_2 is scaled to the sulfuric acid aerosol distribution resulting from the eruption of Mt. Pinatubo. The sulfuric acid aerosol surface area distribution was derived from the SPARC climatology (SPARC, 2006).

By running these three scenarios we are able to compare the relative impact of stratospheric particle injection using TiO_2 compared to sulphate. The benefit of using the Mt. Pinatubo eruption as the sulphate injection scenario is that it provides a natural analogue to proposed climate engineering schemes, and the chemical and dynamical effects of the eruption have been well documented. Telford et al. (2009) have shown that UKCA accurately models the chemical impacts of the Mt. Pinatubo eruption, and the ozone bias is smaller now compared to Telford et al. (2009).

It should be noted that all simulations are nudged to the same observed meteorological conditions, following Telford et al. (2008). In this way we do not take into account the radiative/dynamical feedbacks from any ozone changes resulting from chemical reactions occurring on stratospheric aerosols, allowing just the chemical effects of stratospheric particle injection to be quantified. The results presented here expand on our previous study (Tang et al., 2014c) by including heterogeneous hydrolysis of both N_2O_5 (R1a) and $ClONO_2$ (R1b) on TiO_2. An uptake coefficient of 1.5×10^{-3} is used for R1a (reaction with N_2O_5) on TiO_2 particles as determined by our previous measurement (Tang et al., 2014c). An uptake coefficient of 1.5×10^{-3} is used for R1b (heterogeneous hydrolysis of $ClONO_2$). Considering errors in measurements, this value agrees with experimental $\gamma(ClONO_2)$, which was determined to be ~1.2×10^{-3} in our work as shown in Table 2.

4 Results& Discussion

4.1 Uptake of $ClONO_2$ onto Pyrex glass

The uptake of $ClONO_2$ onto fresh Pyrex glass wall was determined by measuring the $ClONO_2$ concentrations at five different injection positions. The loss of $ClONO_2$ in the coated-wall flow tube, under the assumption of pseudo first order kinetics, can be described by the Eq. (1):

$$[ClONO_2]_t = [ClONO_2]_0 \cdot \exp(-k_w \cdot t) \quad (1)$$

where $[ClONO_2]_t$ and $[ClONO_2]_0$ are the measured $ClONO_2$ concentrations at the reaction time of t and 0, respectively, and k_w is the wall loss rate (s^{-1}). Two typical datasets of measured $[ClONO_2]$ at five different injector positions are displayed in Figure 3, suggesting that $ClONO_2$ indeed follows the exponential decays, and the slopes of the exponential decays are equal to k_w. The effective (or experimental) uptake coefficient of $ClONO_2$, γ_{eff}, onto the Pyrex wall, can then be calculated from k_w, using Eq. (2) (Howard, 1979; Wagner et al., 2008):

$$\gamma_{eff} = \frac{k_w \cdot d_{tube}}{c(ClONO_2)} \quad (2)$$

where d_{tube} is the inner diameter of the flow tube (3.0 cm) and $c(ClONO_2)$ is the average molecular speed of $ClONO_2$ (25 360 cm s^{-1}). Depletion of $ClONO_2$ close to the wall is caused by the uptake of $ClONO_2$ onto the wall, and thus the effective uptake coefficient is smaller than the true one. This effect can be corrected (Tang et al., 2014b), and true uptake coefficients, γ, are reported in Table 1 together with the corresponding wall loss rates (k_w) and effective uptake coefficients (γ_{eff}).

The uptake coefficients of $ClONO_2$ onto Pyrex glass, as summarized in Table 1, increases from ~5×10^{-6} at 0% RH to ~1.6×10^{-5} at 24% RH by a factor of ~3. Uptake coefficients at higher RH were not determined because the uptake coefficients determined at 24% RH (~1.6×10^{-5}) are very close to the upper limit (~2.3×10^{-5}) which can be measured in this study using the coated-wall flow tube technique due to the gas phase diffusion limit. The RH dependence of $\gamma(ClONO_2)$ for Pyrex glass is further discussed in Section 4.4 together with these reported by Molina et al. (1997) and our measurements on SiO_2 and TiO_2 aerosol particles.

4.2 Reaction of $ClONO_2$ with SiO_2 and TiO_2 particles

The uptake of $ClONO_2$ onto airborne SiO_2 and TiO_2 particles were investigated using an atmospheric pressure aerosol flow tube, in which reactions with the aerosol particles and the wall both contribute to the loss of $ClONO_2$, as shown in Eq. (3):

$$[ClONO_2]_t = [ClONO_2]_0 \cdot \exp[-(k_w + k_a) \cdot t] \quad (3)$$

where $[ClONO_2]_t$ and $[ClONO_2]_0$ are the measured $ClONO_2$ mixing ratios at the reaction times of t and 0 s, and k_w and k_a are the loss rates (s^{-1}) of $ClONO_2$ onto the inner wall of the flow tube and the surface of aerosol particles, respectively. In a typical uptake measurement, the aerosol flow was delivered through a filter, and $[ClONO_2]$ was measured at five different injector positions to determine the wall loss rate (k_w). The filter was then bypassed to deliver aerosol

particles into the flow tube, and the total $ClONO_2$ loss rate (k_w + k_a) in the flow tube was determined. After that, the aerosol flow was passed through the filter to measure k_w again. The variation of k_w determined before and after introducing particles into the flow tube was within the experimental uncertainty of k_w, ensuring that the reactivity of the wall towards $ClONO_2$ remained constant during the uptake measurement. Axial and radical diffusion of $ClONO_2$ could lead to biases in its measured loss rates in a flow tube, and this effect, though very small (<10% in our work), has been corrected (Brown, 1978).

The difference between the $ClONO_2$ loss rates without and with aerosol particles in the flow tube, is equal to the loss rate due to the reaction with surface of aerosol particle (k_a). The effective uptake coefficient of $ClONO_2$ onto aerosol particles, γ_{eff}, is related to k_a by Eq. (4) (Crowley et al., 2010):

$$k_a = 0.25 \cdot \gamma_{eff} \cdot c(ClONO_2) \cdot S_a \quad (4)$$

where S_a is the aerosol surface area concentration which can be derived from size-resolved number concentrations (as shown in Figure S1) measured by the SMPS. Uptake of $ClONO_2$ onto aerosol particles also leads to the depletion of $ClONO_2$ near the particle surface and so the effective uptake coefficient is smaller than the true uptake coefficient. This effect, which can be corrected using the method described elsewhere (Tang et al., 2014b), is only a few percent in this study as the particle diameters are <1 μm and the uptake coefficient is relatively small (~1×10^{-3}).

Two typical decays of $ClONO_2$ in the aerosol flow tube without and with SiO_2/TiO_2 aerosol particles in the flow tube are shown in Figure 4. For a majority of experiments, efforts were made to generate enough aerosol particles so that k_a+k_w was significantly different to k_w. It is evident from Figure 4 that the loss of $ClONO_2$ is significantly faster with TiO_2/SiO_2 particles in the flow tube than without aerosols. We acknowledge that the measured k_a and therefore our reported γ in this study have quite large uncertainties. This is because the uptake

coefficients of $ClONO_2$ are very small and the surface area of the wall is ~1000 larger than that of aerosol particles. This is the first time that heterogeneous reactions of $ClONO_2$ with airborne mineral particles have been investigated.

The uptake coefficients of $ClONO_2$ are ~1.2×10^{-3} for TiO_2 particles, and no difference in $\gamma(ClONO_2)$ at two different RH (7% and 33%) is found. The heterogeneous reaction of $ClONO_2$ with SiO_2 particles was studied at four different RH, with $\gamma(ClONO_2)$ increasing from ~2×10^{-4} at 7% RH to ~5×10^{-4} at 35% RH, reaching a value of ~6×10^{-4} at 59% RH. The uptake coefficients of $ClONO_2$ are summarized in Table 2 for SiO_2 and TiO_2 aerosol particles, together with key experimental conditions. It should be pointed out that our measurements were carried out with $ClONO_2$ mixing ratios of several hundred ppbv, significantly higher than those found in the lower stratosphere. Therefore, our measurements could underestimate $\gamma(ClONO_2)$ under stratospheric conditions. In a few measurements in which the SiO_2 aerosol concentrations were relatively low, the total $ClONO_2$ loss rate ($k_w + k_a$) was not different from its wall loss rate (k_w) within the experimental uncertainty. In this case, only the upper limit of k_a (and thus γ) can be estimated, which is reported here as the standard deviation of k_w. The first three of the four uptake coefficients at (17±2)% RH for SiO_2 aerosol particles, tabulated in Table 2, fall into this category. $\gamma(ClONO_2)$ on SiO_2 aerosol particles is around two orders of magnitude larger than that on Pyrex glass. One explanation for such a large difference is that SiO_2 particles used in our work are porous (Tang et al., 2014a) and therefore the surface area which is actually available for the $ClONO_2$ uptake is much larger than that calculated using the mobility diameters. In our previous study (Tang et al., 2014a) we have found that for SiO_2 particles, $\gamma(N_2O_5)$ calculated using the mobility diameter based surface area are a factor of 40 larger than those calculated using the BET surface area. Another reason is that the composition of SiO_2 is different from Pyrex.

4.3 Effects of RH

The RH dependence of $\gamma(ClONO_2)$ for Pyrex glass is plotted in Figure 5 and exhibits a positive dependence on RH, with $\gamma(ClONO_2)$ increased by a factor of ~3 when RH increases from 0% to 24%. Previous studies (Hanson and Ravishankara, 1991; Hanson and Ravishankara, 1994; Zhang et al., 1994; Hanson, 1998) have shown that $\gamma(ClONO_2)$ for aqueous H_2SO_4 solution strongly depends on water content in the solution and it decreases from ~0.1 for 40% H_2SO_4 to ~1×10^{-4} for 75% H_2SO_4 at 200-200 K, by a factor of ~1000. It is suggested that the heterogeneous uptake of $ClONO_2$ by aqueous H_2SO_4 solution proceeds via direct and acid-catalysed hydrolysis (Robinson et al., 1997; Shi et al., 2001; Ammann et al., 2013). One may expect that $\gamma(ClONO_2)$ for Pyrex glass will increase with RH. This is also supported by the water adsorption isotherm on Pyrex glass particles (Chikazawa et al., 1984), showing that the amount of adsorbed water on Pyrex surface displays a substantial increase at 20% RH compared to that at 0% RH. However, the results reported by Chikazawa et al. (1984) are presented graphically and thus impede us from a more quantitative discussion on the effect of RH and surface-adsorbed water on uptake of $ClONO_2$ by Pyrex surface.

One can then expect that $\gamma(ClONO_2)$ may also increase with RH for the reaction with SiO_2 and TiO_2 aerosol particles, since the amount of water adsorbed on these two types of particles also increase with RH (Goodman et al., 2001). Inspection of the data listed in Table 2 reveals that $\gamma(ClONO_2)$ for SiO_2 particle increases from ~2×10^{-4} at 7% RH to ~6×10^{-4} at 59% RH, and this is consistent with the large increase of adsorbed water on SiO_2 surface, from around half a monolayer at ~7% RH to two monolayers at 60% RH (Goodman et al., 2001), as shown in Figure S2. The uptake coefficients of $ClONO_2$ were measured to be ~1.2×10^{-3} for TiO_2 at 7% and 33% RH, with no significant difference found at these two different RH. We expect that further increase in RH will lead to larger $\gamma(ClONO_2)$ for TiO_2, and future studies at higher RH are needed to better understand the RH effects.

At similar RH (7% and 33%), $\gamma(ClONO_2)$ for TiO_2 are significantly larger than those for SiO_2. This may be explained by the larger amount of adsorbed water on TiO_2 at low and medium RH compared to SiO_2 as shown in Figure S2. It is interesting to note that the uptake of N_2O_5 shows different behaviour, i.e. $\gamma(N_2O_5)$ for SiO_2 (Tang et al., 2014a) are significantly larger than that for TiO_2 at similar RH. This may indicate that a different mechanism controls N_2O_5 uptake by mineral surfaces. However, mechanistic explanations of the different heterogeneous reactivities of N_2O_5 and $ClONO_2$ on TiO_2 and SiO_2 surface at the molecular level cannot be derived from our data.

4.4 Comparison with previous work

We find that in the absence of HCl, $\gamma(ClONO_2)$ is around 1.2×10^{-3} for TiO_2 aerosol particles and $<1\times10^{-3}$ for SiO_2 aerosol particles at room temperature. Using the coated-wall flow tube technique, Molina et al. (1997) investigated the uptake of $ClONO_2$ onto the inner wall of an Al_2O_3 tube, α-Al_2O_3 particles, and the inner wall of a Pyrex glass tube, in the presence of $(1\text{-}10)\times10^{-6}$ Torr HCl at 200-220 K. Uptake coefficients of ~0.02 were reported for all the three types of surface (including Pyrex glass), over a factor of 1000 larger than $\gamma(ClONO_2)$ for Pyrex glass determined in our present work. The large difference in $\gamma(ClONO_2)$ reported by the two studies is likely due to the co-presence of HCl (1×10^{-6}-1×10^{-5} Torr) in the experiments of Molina et al. (1997), while no HCl was present in our work. Heterogeneous reactions of $ClONO_2$ proceed via direct and acid-catalysed hydrolysis (Robinson et al., 1997; Shi et al., 2001; Ammann et al., 2013), and numerous previous studies have confirmed that the presence of HCl in the gas phase (and thus partitioning into or adsorption onto the condensed phases) promotes the uptake of $ClONO_2$ by H_2SO_4 solution, ice, and nitric acid trihydrate (NAT), as summarized by Crowley et al. (2010), Sander et al. (2011) and Ammann et al. (2013). Temperature may also play a role since measurements were carried out at 200-220 K by Molina et al. (1997) and at ~296 K in our study.

Considering the importance of HCl in the $ClONO_2$ uptake and its abundance in the stratosphere, it will be important to systematically measure $\gamma(ClONO_2)$ for SiO_2/TiO_2 in the presence of HCl over a broad HCl concentration and temperature range relevant for lower stratosphere.

5 Implication for stratospheric particle injection

Injection of TiO_2 into the stratosphere will provide additional surface area for the heterogeneous reactions of N_2O_5 (R1a) and $ClONO_2$ (R1b, R1c). There are several important types of particles naturally present in the stratosphere (Solomon et al., 1999), including sulfuric acid, ice, and nitric acid trihydrate (NAT), and their interaction with $ClONO_2$ has been well characterised (Crowley et al., 2010; Ammann et al., 2013; Burkholder et al., 2015). Comparing $\gamma(ClONO_2)$ for TiO_2 particles with these other stratospherically relevant surfaces can provide a first order estimate of their relative importance.

The uptake of $ClONO_2$ on H_2SO_4 acid particles is strongly influenced by temperature and the water content in the particles (Shi et al., 2001; Ammann et al., 2013; Burkholder et al., 2015): $\gamma(ClONO_2)$ are $<2\times10^{-3}$ for 65wt% H_2SO_4 particles and $<2\times10^{-4}$ for 75wt% H_2SO_4 particles. The global distribution of $\gamma(ClONO_2)$ calculated for sulfuric acid particles in the stratosphere is shown in the supporting information (Figure S3), suggesting that $\gamma(ClONO_2)$ is lower on TiO_2 particles than on sulfuric acid particles in the lower stratosphere. The uptake coefficient of $ClONO_2$ for water ice shows a negative dependence on temperature, with $\gamma(ClONO_2)$ of ~0.1 at ~200 K (Crowley et al., 2010; Burkholder et al., 2015), around a factor of 100 larger than that for TiO_2 particles at room temperature. $\gamma(ClONO_2)$ for water-rich nitric acid trihydrate (NAT), another important component for polar stratospheric clouds, increases strongly with temperature, with $\gamma(ClONO_2)$ of 3.0×10^{-3} at 200 K, 6.0×10^{-3} at 210 K, and 1.14×10^{-2} at 220 K (Crowley et al., 2010).

While the background burden of stratospheric aerosol is low, volcanic eruptions and deliberate stratospheric particle injection for climate engineering purposes have the potential to significantly increase the available surfaces for heterogeneous reactions. In our current work, three simulations were performed, one representing a low background loading of stratospheric sulphate (<1 Tg) aerosols (S1), a second representing the eruption of Mt. Pinatubo (S2) and a third representing an instantaneous injection of 10 Tg of TiO_2 (S3). SiO_2 particle injection is not considered in our modelling study because the refractive index of SiO_2 is significantly smaller than TiO_2 (Pope et al., 2012). Two heterogeneous reactions on TiO_2 particles, i.e. heterogeneous hydrolysis of N_2O_5 (R1a) and $ClONO_2$ (R1b), were included in the simulation: a value of 1.5×10^{-3} was used for $\gamma(N_2O_5)$, as measured in our previous work (Tang et al., 2014c), and $\gamma(ClONO_2)$ was also set to 1.5×10^{-3}, based on the measurement reported in our current study. All three simulations were nudged to observed meteorology from December 1990 to January 1993. By comparing the TiO_2 injection (S3) with the Mt. Pinatubo eruption (S2) we are able to quantify the relative impacts of TiO_2 and sulphuric acid injection on stratospheric chemistry. Results in this section are presented as annual means for the year 1992.

Similar to our previous study (Tang et al., 2014c), we have found that injection of TiO_2 (S3) has a much smaller impact on stratospheric N_2O_5 concentrations than the eruption of Mt. Pinatubo (S2). N_2O_5 mixing ratios are significantly reduced in S2 compared to S1 from 10-30 km, with concentrations reduced by >80% throughout most of this region. For comparison, after TiO_2 injection (S3) N_2O_5 concentrations are reduced over a much smaller altitude range (15-25 km) and to a lesser degree, with ~20% reductions in the tropics and up to 60% reductions in the high latitudes. The relative effects of TiO_2 injection compared to sulphate injection on N_2O_5 mixing ratios is calculated as the difference between S3 and S2. As shown in Figure 6, throughout most of the stratosphere N_2O_5 mixing ratios remain higher under S3 than S2.

552 Under both particle injection scenarios (S2 and S3), stratospheric ClOx mixing ratios are
553 increased compared to S1 due to the activation of $ClONO_2$ through heterogeneous reactions.
554 However, Figure 7 suggests that ClOx mixing ratios are up to 40% lower in the tropical lower
555 stratosphere following the injection of TiO_2 aerosols compared to sulphate. This is driven in
556 part by the lower surface area density of TiO_2 compared to sulphate, but also due to the
557 difference in uptake coefficients. The uptake coefficient of $ClONO_2$ onto sulphate is
558 temperature dependent, and our measurements suggest that the uptake coefficient onto fresh
559 TiO_2 is smaller than that for sulphate below ~215 K. Throughout much of the tropical lower
560 stratosphere where maximum aerosol surface area density is found in both S2 and S3,
561 temperatures are below ~220 K and therefore the uptake coefficient is lower for TiO_2 than
562 sulphate (as shown by Figure S3 in the supporting information), leading to reduced chlorine
563 activation. Previous studies have investigated the influence of temperature on the
564 heterogeneous reactions of mineral particles with a few other trace gases, including HCOOH
565 (Wu et al., 2012), H_2O_2 (Romanias et al., 2012) and OH radicals (Bedjanian et al., 2013), and
566 found that the measured uptake coefficients varied only by a factor of 2-3 or less across a wide
567 temperature range. However, it is unclear whether temperature would have a significant effect
568 on $\gamma(ClONO_2)$ for TiO_2 particles, and therefore our simulated impact of heterogeneous reaction
569 of $ClONO_2$ with TiO_2 on stratospheric chemistry may have large uncertainties. The sensitivity
570 of simulated stratospheric compositions to $\gamma(ClONO_2)$ for TiO_2 particles will be investigated
571 in a following paper.

572 The relative difference in ozone mixing ratios following TiO_2 injection (S3) compared
573 with the eruption of Mt. Pinatubo (S2) is shown in Figure 8. Ozone mixing ratios in the lower
574 stratosphere decrease as a result of both TiO_2 and sulphate injection, with largest decreases
575 seen at high latitudes. In terms of annual means, the magnitude of this ozone response is
576 comparable between the two simulations, with a maximum of ~3% in the tropics and ~7% at

high latitudes. In contrast, ozone mixing ratios at the altitude of 25 km increase following the eruption of Mt. Pinatubo (S2), but show no significant change upon TiO_2 injection (S3). This is consistent with the much faster uptake of N_2O_5 onto sulphate aerosols and the resultant stratospheric NOx loss and decreases in the rates of catalytic ozone destruction at these altitudes.

The results presented here indicate that there is little difference in stratospheric ozone concentrations between injection of TiO_2 and sulphate aerosols when R1a and R1b are considered on TiO_2. While TiO_2 injection (S3) leads to less ClOx activation and ozone destruction in the lowermost stratosphere, the reduced depletion of N_2O_5 and NOx in the middle stratosphere leads to decreased ozone mixing ratios compared to sulphate injection (S2). The total column ozone differences between S3 and S2 are within ±2.5%, indicating that there is no significant difference in vertically integrated ozone abundancies and solar UV amounts reaching the surface. However, more work is required to establish additional kinetic data for heterogeneous reactions of TiO_2.

6 Conclusions and outlook

Minerals with high refractive indices, such as TiO_2, have been proposed as possible materials used for stratospheric particle injection for climate engineering (Pope et al., 2012). However, kinetic data of their heterogeneous reactions with important reactive trace gases (e.g., N_2O_5 and $ClONO_2$) in the stratosphere are lacking, impeding us from a reliable assessment of the impacts of mineral particle injection on stratospheric ozone in particular and stratosphere chemistry in general. In our current work, using an atmospheric pressure aerosol flow tube, we have investigated the heterogeneous reaction of $ClONO_2$ with TiO_2 and SiO_2 aerosol particles at room temperature and at different RH. The uptake coefficient, $\gamma(ClONO_2)$, was ~1.2×10^{-3} at 7% and 33% RH for TiO_2 particles, with no significant difference observed at these two RH; for SiO_2 particles, $\gamma(ClONO_2)$ increases from ~2×10^{-4} at 7% RH to ~6×10^{-4} at 59%, showing a

positive dependence on RH. Therefore, it can be concluded that under similar conditions for the RH range covered in this work, TiO_2 shows higher heterogeneous reactivity than SiO_2 towards $ClONO_2$. Compared to sulfuric acid particles in the lower stratosphere, the heterogeneous reactivity towards $ClONO_2$ is lower for TiO_2 particles. In addition, the heterogeneous uptake of $ClONO_2$ by Pyrex glass was also studied, with $\gamma(ClONO_2)$ increasing from ~4.5×10^{-6} at 0% RH to ~1.6×10^{-5} at 24% RH.

Using the UKCA chemistry-climate model with nudged meteorology, we have constructed a scenario to assess the impact of TiO_2 particle injection on stratospheric chemistry. In this scenario TiO_2 aerosol particles are distributed in the stratosphere in such a way that TiO_2 particle injection is assumed to produce a radiative effect similar to that of Mt. Pinatubo eruption, following Pope et al. (2012). Heterogeneous reactions of N_2O_5 and $ClONO_2$ with TiO_2 aerosol particles, both with an uptake coefficient of 1.5×10^{-3} based on our previous (Tang et al., 2014c) and current laboratory experiments, were included in the simulation. It is found that compared to the eruption of Mt. Pinatubo, the TiO_2 injection has a much smaller impact on N_2O_5 in the stratosphere, although significant reduction (20-60% compared to the background scenario without additional particle injection) in stratospheric N_2O_5 also occurs. Compared to the background scenario, both TiO_2 injection and the Mt. Pinatubo eruption scenarios lead to increased stratospheric ClOx mixing ratios, and the ClOx mixing ratios are lower for the TiO_2 injection than the Mt. Pinatubo eruption. Both TiO_2 injection and the Mt. Pinatubo eruption results in significant ozone depletion in the lower stratosphere, with largest decreases occurring at high latitudes. In comparison with Mt. Pinatubo eruption, TiO_2 injection causes less ClOx activation and less ozone destruction in the lowermost stratosphere, while the reduced depletion of N_2O_5 and NOx in the middle stratosphere results in decreased ozone levels. Overall, our simulation results suggest that there is no significant difference (within ±2.5%) in the vertically integrated ozone abundancies between TiO_2 injection and Mt. Pinatubo eruption.

It should be emphasized that heterogeneous chemistry of TiO_2 included in our current modelling study is not complete. One example is the heterogeneous reaction of $ClONO_2$ with HCl (R1c) on/in the particles. An uptake coefficient of 0.02 was reported for the heterogeneous reaction of $ClONO_2$ with HCl on Al_2O_3 particles (Molina et al., 1997), and it is reasonable to assume that this reaction may also be quite fast on TiO_2 particles. The heterogeneous reaction of $ClONO_2$ with HCl on TiO_2 particles, with an uptake coefficient assumed to be the same as that on Al_2O_3 surface (i.e. 0.02) as reported by Molina et al. (1997), has been included in further simulations, and the results will be reported and discussed in a following paper. Other reactions, including the heterogeneous reaction of HOCl (Molina et al., 1996; Solomon, 1999) and a range of heterogeneous photochemical reactions (Chen et al., 2012; George et al., 2015), may also be important and thus deserve further laboratory and modeling investigation. In this work we have only considered heterogeneous chemistry of fresh TiO_2 particles. If injected into the stratosphere, TiO_2 particles would be coated with H_2SO_4, NAT, water ice, etc., and heterogeneous reactivity of coated TiO_2 particles could be very different from fresh particles. This important issue should be addressed by further laboratory and modeling studies.

Our nudged modeling simulations, designed to focus on chemistry effects, do not take into account feedbacks between radiative effects, atmospheric dynamics, and chemistry. Several recent studies have assessed the impact of high latitude stratospheric ozone depletion using the UKCA model (Braesicke et al., 2013; Keeble et al., 2014) and have shown that interactive feedbacks can affect stratospheric temperatures, the strength of the Brewer-Dobson circulation, the longevity of polar vortices and surface climate. By nudging the model to observed meteorology during the Mt. Pinatubo eruption these feedbacks are implicitly included in the sulphate injection scenario. However, while we have chosen a TiO_2 loading to give the same surface radiative response as the Mt. Pinatubo eruption, the stratospheric radiative impacts may differ. In order to fully understand the true impact of stratospheric particle

injection, both the radiative and chemical effects, and the coupling between these responses, need to be explored further. In addition, before any climate engineering schemes could be considered, much consideration is absolutely obligatory, including, but not limited to, technical, socioeconomic, political, environmental, and ethical feasibilities.

Acknowledgement

Financial support provided by EPSRC Grant EP/I01473X/1 and the Isaac Newton Trust (Trinity College, University of Cambridge, U.K.) is acknowledged. We thank NCAS-CMS for modelling support. Model integrations have been performed using the ARCHER UK National Supercomputing Service. We acknowledge the ERC for support through the ACCI project (project number: 267760). M. J. T. would like to thank the CAS Pioneer Hundred Talents program and State Key Laboratory of Organic Geochemistry for providing starting grants.

Reference

Ammann, M., Cox, R. A., Crowley, J. N., Jenkin, M. E., Mellouki, A., Rossi, M. J., Troe, J., and Wallington, T. J.: Evaluated kinetic and photochemical data for atmospheric chemistry: Volume VI - heterogeneous reactions with liquid substrates, Atmos. Chem. Phys., 12, 8045-8228, 2013.

Anderson, L. C., and Fahey, D. W.: Studies with $ClONO_2$: Thermal-dissociation rate and catalytic conversion to NO using an NO/O_3 chemi-luminescence detector, J. Phys. Chem., 94, 644-652, 1990.

Ball, S. M., Fried, A., Henry, B. E., and Mozurkewich, M.: The hydrolysis of $ClONO_2$ on sub-micron liquid sulfuric acid aerosol, Geophys. Res. Lett., 25, 3339-3342, 1998.

Ballard, J., Johnston, W. B., Gunson, M. R., and Wassell, P. T.: Absolute absorption coefficients of $ClONO_2$ infrared bands at stratospheric temperatures, J. Geophys. Res.-Atmos, 93, 1659-1665, 1988.

Bannan, T. J., Booth, A. M., Bacak, A., Muller, J. B. A., Leather, K. E., Le Breton, M., Jones, B., Young, D., Coe, H., Allan, J., Visser, S., Slowik, J. G., Furger, M., Prévôt, A. S. H., Lee, J., Dunmore, R. E., Hopkins, J. R., Hamilton, J. F., Lewis, A. C., Whalley, L. K., Sharp, T., Stone, D., Heard, D. E., Fleming, Z. L., Leigh, R., Shallcross, D. E., and Percival, C. J.: The first UK measurements of nitryl chloride using a chemical ionization mass spectrometer in central London in the summer of 2012, and an investigation of the role of Cl atom oxidation, J. Geophys. Res.-Atmos, 120, 5638-5657, 2015.

Bedjanian, Y., Romanias, M. N., and El Zein, A.: Interaction of OH Radicals with Arizona Test Dust: Uptake and Products, J. Phys. Chem. A, 117, 393-400, 2013.

Braesicke, P., Keeble, J., Yang, X., Stiller, G., Kellmann, S., Abraham, N. L., Archibald, A., Telford, P., and Pyle, J. A.: Circulation anomalies in the Southern Hemisphere and ozone changes, Atmos. Chem. Phys., 13, 10677-10688, 2013.

Brown, R. L.: Tubular flow reactors with first-order kinetics, J. Res. Nat. Bur. Standards., 83, 1-8, 1978.

Burkholder, J. B., Sander, S. P., Abbatt, J. P. D., Barker, J. R., Huie, R. E., Kolb, C. E., Kurylo, M. J., Orkin, V. L., Wilmouth, D. M., and Wine, P. H.: Chemical Kinetics and Photochemical Data for Use in Atmospheric Studies, Evaluation No. 18, JPL Publication 15-10, Jet Propulsion Lab., Pasadena, CA, 2015.

Chen, H. H., Nanayakkara, C. E., and Grassian, V. H.: Titanium Dioxide Photocatalysis in Atmospheric Chemistry, Chem. Rev., 112, 5919-5948, 2012.

Chikazawa, M., Kanazawa, T., and Yamaguchi, T.: The Role of Adsorbed Water on Adhesion Force of Powder Particles, KONA, 2, 54-61, 1984.

Chipperfield, M. P.: Multiannual simulations with a three-dimensional chemical transport model, J. Geophys. Res.-Atmos, 104, 1781-1805, 1999.

Crowley, J. N., Ammann, M., Cox, R. A., Hynes, R. G., Jenkin, M. E., Mellouki, A., Rossi, M. J., Troe, J., and Wallington, T. J.: Evaluated Kinetic and Photochemical Data for Atmospheric Chemistry: Volume V - Heterogeneous Reactions on Solid Substrates, Atmos. Chem. Phys., 10, 9059-9223, 2010.

Crutzen, P. J.: Albedo enhancement by stratospheric sulfur injections: A contribution to resolve a policy dilemma?, Clim. Change, 77, 211-219, 2006.

Danilin, M. Y., Shia, R. L., Ko, M. K. W., Weisenstein, D. K., Sze, N. D., Lamb, J. J., Smith, T. W., Lohn, P. D., and Prather, M. J.: Global stratospheric effects of the alumina emissions by solid-fueled rocket motors, J. Geophys. Res.-Atmos, 106, 12727-12738, 2001.

Davidson, J. A., Cantrell, C. A., Shetter, R. E., McDaniel, A. H., and Calvert, J. G.: Absolute infrared absorption cross sections for $ClONO_2$ at 296 and 223 K, J. Geophys. Res.-Atmos., 92, 10921-10925, 1987.
Dee, D. P., Uppala, S. M., Simmons, A. J., Berrisford, P., Poli, P., Kobayashi, S., Andrae, U., Balmaseda, M. A., Balsamo, G., Bauer, P., Bechtold, P., Beljaars, A. C. M., van de Berg, L., Bidlot, J., Bormann, N., Delsol, C., Dragani, R., Fuentes, M., Geer, A. J., Haimberger, L., Healy, S. B., Hersbach, H., Holm, E. V., Isaksen, L., Kallberg, P., Kohler, M., Matricardi, M., McNally, A. P., Monge-Sanz, B. M., Morcrette, J. J., Park, B. K., Peubey, C., de Rosnay, P., Tavolato, C., Thepaut, J. N., and Vitart, F.: The ERA-Interim reanalysis: configuration and performance of the data assimilation system, Q. J. R. Meteorol. Soc., 137, 553-597, 2011.
Deiber, G., George, C., Le Calvé, S., Schweitzer, F., and Mirabel, P.: Uptake study of $ClONO_2$ and $BrONO_2$ by Halide containing droplets, Atmos. Chem. Phys., 4, 1291-1299, 2004.
Dutton, E. G., and Christy, J. R.: Solar radiative forcing at selected locations and evidence for global lower tropospheric cooling following the eruptions of El Chichón and Pinatubo, Geophys. Res. Lett., 19, 2313-2316, 1992.
Fahey, D. W., Eubank, C. S., Hubler, G., and Fehsenfeld, F. C.: A Calibrated Source of N_2O_5, Atmos. Environ., 19, 1883-1890, 1985.
Fahey, D. W., Kawa, S. R., Woodbridge, E. L., Tin, P., Wilson, J. C., Jonsson, H. H., Dye, J. E., Baumgardner, D., Borrmann, S., Toohey, D. W., Avallone, L. M., Proffitt, M. H., Margitan, J., Loewenstein, M., Podolske, J. R., Salawitch, R. J., Wofsy, S. C., Ko, M. K. W., Anderson, D. E., Schoeberl, M. R., and Chan, K. R.: In situ measuremnet constraining the role of sulfate aerosol in midelatitude ozone depletion, Nature, 363, 509-514, 1993.
Fernandez, M. A., Hynes, R. G., and Cox, R. A.: Kinetics of $ClONO_2$ reactive uptake on ice surfaces at temperatures of the upper troposphere, J. Phys. Chem. A, 109, 9986-9996, 2005.
Ferraro, A. J., Highwood, E. J., and Charlton-Perez, A. J.: Stratospheric heating by potential geoengineering aerosols, Geophys. Res. Lett., 38, L24706, 10.1029/2011GL049761, 2011.
Finlayson-Pitts, B. J., Ezell, M. J., and Pitts, J. N.: Formation of Chemically Active Chlorine Compounds by Reactions of Atmospheric NaCl Particles with Gaseous N_2O_5 and $ClONO_2$, Nature, 337, 241-244, 1989.
George, C., Ammann, M., D'Anna, B., Donaldson, D. J., and Nizkorodov, S. A.: Heterogeneous Photochemistry in the Atmosphere, Chem. Rev., 115, 4218-4258, 2015.
Ginoux, P., Prospero, J. M., Gill, T. E., Hsu, N. C., and Zhao, M.: Global-scale Attribution of Anthropogenic and Natural Dust Sources and Their Emission Rates Based on MODIS Deep Blue Aerosol Products, Rev. Geophys., 50, RG3005, doi: 3010.1029/2012RG000388, 2012.
Goodman, A. L., Bernard, E. T., and Grassian, V. H.: Spectroscopic Study of Nitric Acid and Water Adsorption on Oxide Particles: Enhanced Nitric Acid Uptake Kinetics in the Presence of Adsorbed Water, J. Phys. Chem. A, 105, 6443-6457, 2001.
Guo, S., Bluth, G. J. S., Rose, W. I., Watson, I. M., and Prata, A. J.: Re-evaluation of SO2 release of the 15 June 1991 Pinatubo eruption using ultraviolet and infrared satellite sensors, Geochem. Geophys. Geosyst., 5, Q04001, doi: 04010.01029/02003GC000654, 2004.
Hanson, D. R., and Ravishankara, A. R.: The reaction probabilities of $ClONO_2$ and N_2O_5 on polar stratospheric cloud materials, J. Geophys. Res.-Atmos., 96, 5081-5090, 1991.
Hanson, D. R., and Ravishankara, A. R.: Reactive uptake of $ClNO_2$ onto sulfuric-acid due to reaction with HCl and H_2O, J. Phys. Chem., 98, 5728-5735, 1994.
Hanson, D. R., and Lovejoy, E. R.: The Reaction of $ClONO_2$ with Submicrometer Sulfuric-Acid Aerosol, Science, 267, 1326-1328, 1995.
Hanson, D. R.: Reaction of $ClONO_2$ with H_2O and HCl in sulfuric acid and HNO_3/H2SO_4/H_2O mixtures, J. Phys. Chem. A, 102, 4794-4807, 1998.

Hauglustaine, D. A., Hourdin, F., Jourdain, L., Filiberti, M. A., Walters, S., Lamarque, J. F., and Holland, E. A.: Interactive chemistry in the Laboratoire de Meteorologie Dynamique general circulation model: Description and background tropospheric chemistry evaluation, J. Geophys. Res.-Atmos., 109, D04314, doi: 04310.01029/02003jd003957, 2004.
Hinds, W. C.: Aerosol techniques: properties, behavior, and measurement if airborne particles, John Wiley& Sons. Inc., New York, 1996.
Howard, C. J.: Kinetic Measurements Using Flow Tubes, J. Phys. Chem., 83, 3-9, 1979.
Jackman, C. H., Considine, D. B., and Fleming, E. L.: A global modeling study of solid rocket aluminum oxide emission effects on stratospheric ozone, Geophys. Res. Lett., 25, 907-910, 1998.
Jeuken, A. B. M., Siegmund, P. C., Heijboer, L. C., Feichter, J., and Bengtsson, L.: On the potential of assimilating meteorological analyses in a global climate model for the purpose of model validation, J. Geophys. Res.-Atmos., 101, 16939-16950, 1996.
Jones, A. C., Haywood, J. M., and Jones, A.: Climatic impacts of stratospheric geoengineering with sulfate, black carbon and titania injection, Atmos. Chem. Phys., 16, 2843-2862, 2016.
Kebede, M. A., Scharko, N. K., Appelt, L. E., and Raff, J. D.: Formation of Nitrous Acid during Ammonia Photooxidation on TiO2 under Atmospherically Relevant Conditions, J. Phys. Chem. Lett., 4, 2618-2623, 2013.
Keeble, J., Braesicke, P., Abraham, N. L., Roscoe, H. K., and Pyle, J. A.: The impact of polar stratospheric ozone loss on Southern Hemisphere stratospheric circulation and climate, Atmos. Chem. Phys., 14, 13705-13717, 2014.
Kravitz, B., Robock, A., Forster, P. M., Haywood, J. M., Lawrence, M. G., and Schmidt, H.: An overview of the Geoengineering Model Intercomparison Project (GeoMIP), J. Geophys. Res.-Atmos., 118, 13103-13107, 2013.
Lawler, M. J., Sander, R., Carpenter, L. J., Lee, J. D., von Glasow, R., Sommariva, R., and Saltzman, E. S.: HOCl and Cl_2 observations in marine air, Atmos. Chem. Phys., 11, 7617-7628, 2011.
Lee, S. H., Leard, D. C., Zhang, R. Y., Molina, L. T., and Molina, M. J.: The HCl+$ClONO_2$ reaction rate on various water ice surfaces, Chem. Phys. Lett., 315, 7-11, 1999.
Liao, J., Huey, L. G., Liu, Z., Tanner, D. J., Cantrell, C. A., Orlando, J. J., Flocke, F. M., Shepson, P. B., Weinheimer, A. J., Hall, S. R., Ullmann, K., Beine, H. J., Wang, Y., Ingall, E. D., Stephens, C. R., Hornbrook, R. S., Apel, E. C., Riemer, D., Fried, A., Mauldin Iii, R. L., Smith, J. N., Staebler, R. M., Neuman, J. A., and Nowak, J. B.: High levels of molecular chlorine in the Arctic atmosphere, Nature Geosci., 7, 91-94, 2014.
McCormick, M. P., Thomason, L. W., and Trepte, C. R.: Atmospheric effects of the Mt Pinatubo eruption, Nature, 373, 399-404, 1995.
Molina, L. T., Spencer, J. E., and Molina, M. J.: The rate constant for the reaction of $O(^3P)$ atoms with $ClONO_2$, Chem. Phys. Lett., 45, 158-162, 1977.
Molina, M. J., Molina, L. T., and Kolb, C. E.: Gas-phase and heterogeneous chemical kinetics of the troposphere and stratosphere, Annu. Rev. Phys. Chem., 47, 327-367, 1996.
Molina, M. J., Molina, L. T., Zhang, R. Y., Meads, R. F., and Spencer, D. D.: The reaction of $ClONO_2$ with HCl on aluminum oxide, Geophys. Res. Lett., 24, 1619-1622, 1997.
Morgenstern, O., Braesicke, P., O'Connor, F. M., Bushell, A. C., Johnson, C. E., Osprey, S. M., and Pyle, J. A.: Evaluation of the new UKCA climate-composition model – Part 1: The stratosphere, Geosci. Model Dev., 2, 43-57, 2009.
O'Connor, F. M., Johnson, C. E., Morgenstern, O., Abraham, N. L., Braesicke, P., Dalvi, M., Folberth, G. A., Sanderson, M. G., Telford, P. J., Voulgarakis, A., Young, P. J., Zeng, G.,

Collins, W. J., and Pyle, J. A.: Evaluation of the new UKCA climate-composition model – Part 2: The Troposphere, Geosci. Model Dev., 7, 41-91, 2014.
Osthoff, H. D., Roberts, J. M., Ravishankara, A. R., Williams, E. J., Lerner, B. M., Sommariva, R., Bates, T. S., Coffman, D., Quinn, P. K., Dibb, J. E., Stark, H., Burkholder, J. B., Talukdar, R. K., Meagher, J., Fehsenfeld, F. C., and Brown, S. S.: High levels of nitryl chloride in the polluted subtropical marine boundary layer, Nature Geosci., 1, 324-328, 2008.
Phillips, G. J., Tang, M. J., Thieser, J., Brickwedde, B., Schuster, G., Bohn, B., Lelieveld, J., and Crowley, J. N.: Significant concentrations of nitryl chloride observed in rural continental Europe associated with the influence of sea salt chloride and anthropogenic emissions, Geophys. Res. Lett., 39, L10811, 10.1029/2012gl051912, 2012.
Pope, F. D., Braesicke, P., Grainger, R. G., Kalberer, M., Watson, I. M., Davidson, P. J., and Cox, R. A.: Stratospheric aerosol particles and solar-radiation management, Nature Clim. Change, 2, 713-719, 2012.
Renard, J. J., and Bolker, H. I.: The chemistry of chlorine monoxide (dichlorine monoxide), Chem. Rev., 76, 487-508, 1976.
Riedel, T. P., Bertram, T. H., Crisp, T. A., Williams, E. J., Lerner, B. M., Vlasenko, A., Li, S.-M., Gilman, J., de Gouw, J., Bon, D. M., Wagner, N. L., Brown, S. S., and Thornton, J. A.: Nitryl Chloride and Molecular Chlorine in the Coastal Marine Boundary Layer, Environ. Sci. Technol., 46, 10463-10470, 2012.
Robinson, G. N., Worsnop, D. R., Jayne, J. T., Kolb, C. E., and Davidovits, P.: Heterogeneous uptake of $ClONO_2$ and N_2O_5 by sulfuric acid solutions, J. Geophys. Res.-Atmos., 102, 3583-3601, 1997.
Romanias, M. N., El Zein, A., and Bedjanian, Y.: Heterogeneous Interaction of H_2O_2 with TiO_2 Surface under Dark and UV Light Irradiation Conditions, J. Phys. Chem. A, 116, 8191-8200, 2012.
Rouviere, A., Sosedova, Y., and Ammann, M.: Uptake of Ozone to Deliquesced KI and Mixed KI/NaCl Aerosol Particles, J. Phys. Chem. A, 114, 7085-7093, 2010.
Schack, C. J., and Lindahl, C. B.: On the synthesis of chlorine monoxide, Inorg. Nucel. Chem. Lett., 3, 387-389, 1967.
Schmidt, G. A., Ruedy, R., Hansen, J. E., Aleinov, I., Bell, N., Bauer, M., Bauer, S., Cairns, B., Canuto, V., Cheng, Y., Del Genio, A., Faluvegi, G., Friend, A. D., Hall, T. M., Hu, Y. Y., Kelley, M., Kiang, N. Y., Koch, D., Lacis, A. A., Lerner, J., Lo, K. K., Miller, R. L., Nazarenko, L., Oinas, V., Perlwitz, J., Perlwitz, J., Rind, D., Romanou, A., Russell, G. L., Sato, M., Shindell, D. T., Stone, P. H., Sun, S., Tausnev, N., Thresher, D., and Yao, M. S.: Present-day atmospheric simulations using GISS ModelE: Comparison to in situ, satellite, and reanalysis data, Journal of Climate, 19, 153-192, 2006.
Shang, J., Li, J., and Zhu, T.: Heterogeneous Reaction of SO_2 on TiO_2 Particles, Sci. China Chem., 53, 2637-2643, 2010.
Shepherd, J.: Geoengineering the climate: science, governance and uncertainty, The Royal Society, London, UK, 2009.
Shi, Q., Jayne, J. T., Kolb, C. E., Worsnop, D. R., and Davidovits, P.: Kinetic model for reaction of $ClONO_2$ with H_2O and HCl and HOCl with HCl in sulfuric acid solutions, J. Geophys. Res.-Atmos., 106, 24259-24274, 2001.
Simpson, W. R., Brown, S. S., Saiz-Lopez, A., Thornton, J. A., and Glasow, R. v.: Tropospheric Halogen Chemistry: Sources, Cycling, and Impacts, Chem. Rev., 115, 4035-4062, 2015.
Solomon, S.: Stratospheric ozone depletion: A review of concepts and history, Rev. Geophys., 37, 275-316, 1999.
SPARC: Assessment of Stratospheric Aerosol Properties (SPARCR Report No. 4), 2006.

Spicer, C. W., Chapman, E. G., Finlayson-Pitts, B. J., Plastridge, R. A., Hubbe, J. M., Fast, J. D., and Berkowitz, C. M.: Unexpectedly high concentrations of molecular chlorine in coastal air, Nature, 394, 353-356, 1998.
Stull, D. R.: Vapor Pressure of Pure Substances. Organic and Inorganic Compounds, Ind. Eng. Chem., 39, 517-540, 1947.
Takemura, T., Okamoto, H., Maruyama, Y., Numaguti, A., Higurashi, A., and Nakajima, T.: Global three-dimensional simulation of aerosol optical thickness distribution of various origins, J. Geophys. Res.-Atmos., 105, 17853-17873, 2000.
Tang, M. J., Thieser, J., Schuster, G., and Crowley, J. N.: Kinetics and Mechanism of the Heterogeneous Reaction of N_2O_5 with Mineral Dust Particles, Phys. Chem. Chem. Phys., 14, 8551-8561, 2012.
Tang, M. J., Camp, J. C. J., Rkiouak, L., McGregor, J., Watson, I. M., Cox, R. A., Kalberer, M., Ward, A. D., and Pope, F. D.: Heterogeneous Interaction of SiO_2 with N_2O_5: Aerosol Flow Tube and Single Particle Optical Levitation-Raman Spectroscopy Studies, J. Phys. Chem. A, 118, 8817-8827, 2014a.
Tang, M. J., Cox, R. A., and Kalberer, M.: Compilation and Evaluation of Gas Phase Diffusion Coefficients of Reactive Trace Gases in the Atmosphere: Volume 1. Inorganic Compounds, Atmos. Chem. Phys., 14, 9233-9247, 2014b.
Tang, M. J., Telford, P. J., Pope, F. D., Rkiouak, L., Abraham, N. L., Archibald, A. T., Braesicke, P., Pyle, J. A., McGregor, J., Watson, I. M., Cox, R. A., and Kalberer, M.: Heterogeneous reaction of N_2O_5 with airborne TiO_2 particles and its implication for stratospheric particle injection, Atmos. Chem. Phys., 14, 6035-6048, 2014c.
Tang, M. J., Cziczo, D. J., and Grassian, V. H.: Interactions of Water with Mineral Dust Aerosol: Water Adsorption, Hygroscopicity, Cloud Condensation and Ice Nucleation, Chem. Rev., 116, 4205–4259, 2016.
Telford, P., Braesicke, P., Morgenstern, O., and Pyle, J.: Reassessment of causes of ozone column variability following the eruption of Mount Pinatubo using a nudged CCM, Atmos. Chem. Phys., 9, 4251-4260, 2009.
Telford, P. J., Braesicke, P., Morgenstern, O., and Pyle, J. A.: Technical Note: Description and assessment of a nudged version of the new dynamics Unified Model, Atmos. Chem. Phys., 8, 1701-1712, 2008.
Textor, C., Schulz, M., Guibert, S., Kinne, S., Balkanski, Y., Bauer, S., Berntsen, T., Berglen, T., Boucher, O., Chin, M., Dentener, F., Diehl, T., Easter, R., Feichter, H., Fillmore, D., Ghan, S., Ginoux, P., Gong, S., Grini, A., Hendricks, J., Horowitz, L., Huang, P., Isaksen, I., Iversen, I., Kloster, S., Koch, D., Kirkevåg, A., Kristjansson, J. E., Krol, M., Lauer, A., Lamarque, J. F., Liu, X., Montanaro, V., Myhre, G., Penner, J., Pitari, G., Reddy, S., Seland, Ø., Stier, P., Takemura, T., and Tie, X.: Analysis and Quantification of the Diversities of Aerosol Life Cycles within AeroCom, Atmos. Chem. Phys., 6, 1777-1813, 2006.
Thornton, J. A., Kercher, J. P., Riedel, T. P., Wagner, N. L., Cozic, J., Holloway, J., S., Dube, W. P., Wolfe, G. M., Quinn, P. K., Middlebrook, A. M., Alexander, B., and Brown, S. S.: A large atomic chlorine source inferred from mid-continental reactive nitrogen chemistry, Nature, 464, 271-174, 2010.
Tilmes, S., Muller, R., and Salawitch, R.: The sensitivity of polar ozone depletion to proposed geoengineering schemes, Science, 320, 1201-1204, 2008.
Tilmes, S., Mills, M. J., Niemeier, U., Schmidt, H., Robock, A., Kravitz, B., Lamarque, J. F., Pitari, G., and English, J. M.: A new Geoengineering Model Intercomparison Project (GeoMIP) experiment designed for climate and chemistry models, Geosci. Model Dev., 8, 43-49, 2015.

Wagner, C., Hanisch, F., Holmes, N., de Coninck, H., Schuster, G., and Crowley, J. N.: The interaction of N_2O_5 with mineral dust: aerosol flow tube and Knudsen reactor studies, Atmos. Chem. Phys., 8, 91-109, 2008.
Wang, T., Tham, Y. J., Xue, L., Li, Q., Zha, Q., Wang, Z., Poon, S. C. N., Dubé, W. P., Blake, D. R., Louie, P. K. K., Luk, C. W. Y., Tsui, W., and Brown, S. S.: Observations of nitryl chloride and modeling its source and effect on ozone in the planetary boundary layer of southern China, J. Geophys. Res.-Atmos, 121, 2476-2489, 2016.
Weisenstein, D. K., Keith, D. W., and Dykema, J. A.: Solar geoengineering using solid aerosol in the stratosphere, Atmos. Chem. Phys., 15, 11835-11859, 2015.
Wilson, J. C., Jonsson, H. H., Brock, C. A., Toohey, D. W., Avallone, L. M., Baumgardner, D., Dye, J. E., Poole, L. R., Woods, D. C., Decoursey, R. J., Osborn, M., Pitts, M. C., Kelly, K. K., Chan, K. R., Ferry, G. V., Loewenstein, M., Podolske, J. R., and Weaver, A.: In-situe observations of aerosol and chlorine monoxide after the 1991 eruption of Mount-Pinatubo: effect of reactions on sulfate aerosol, Science, 261, 1140-1143, 1993.
Wu, L.-Y., Tong, S.-R., Hou, S.-Q., and Ge, M.-F.: Influence of Temperature on the Heterogeneous Reaction of Formic Acid on α-Al_2O_3, J. Phys. Chem. A, 116, 10390-10396, 2012.
Zhang, R. Y., Jayne, J. T., and Molina, M. J.: Heterogeneous interacyions of $ClONO_2$ and HCl with surlfuric acid tetrehydrate: implications for the stratosphere, J. Phys. Chem., 98, 867-874, 1994.

Tables& Figures

Table 1. Loss rates (k_w), effective uptake coefficients (γ_{ss}), and true uptake coefficients (γ) of $ClONO_2$ onto the inner wall of the Pyrex tube at different relative humidities (RH). Measurements were all carried out with initial $ClONO_2$ mixing ratios of several hundred ppbv.

RH (%)	k_w ($\times10^{-2}$ s^{-1})	γ_{eff}($\times10^{-6}$)	γ ($\times10^{-6}$)
0	3.6±0.2	4.2±0.3	5.1±0.3
	2.9±0.4	3.4±0.5	3.9±0.6
6	4.1±0.1	4.9±0.1	6.2±0.1
	3.7±0.7	4.4±0.8	5.4±1.0
12	4.1±0.3	4.9±0.4	6.2±0.5
17	6.9±0.3	8.2±0.4	13±0.6
	6.4±0.2	7.6±0.2	11±0.4
24	8.1±0.8	9.6±1.0	16±2.0
	8.2±0.3	9.6±0.4	17±0.7

Table 2. Uptake coefficients of $ClONO_2$ onto SiO_2 and TiO_2 aerosol particles at different relative humidities (RH). k_a: loss rate of $ClONO_2$ onto aerosol particle surface; S_a: aerosol surface area concentration; $\gamma(ClONO_2)$: uptake coefficients of $ClONO_2$. Measurements were all carried out with initial $ClONO_2$ mixing ratios of several hundred ppbv.

Particle	RH (%)	k_a ($\times10^{-3}$ s)	S_a ($\times10^{-3}$ cm^2 cm^{-3})	$\gamma(ClONO_2)$ ($\times10^{-4}$)
SiO_2	7±1	4.1±2.5	2.80±0.02	2.3±1.4
	7±1	3.4±3.2	2.78±0.05	1.9±1.8
	17±2	<5.1 [a]	1.08±0.08	<7.5 [a]
	17±2	<5.4 [a]	1.28±0.07	<6.7 [a]
	17±2	<7.3 [a]	1.78±0.09	<6.5 [a]
	17±2	6.5±4.2	2.08±0.06	4.9±3.2
	35±4	6.3±3.1	2.34±0.08	4.2±2.1
	35±4	13.1±4.7	2.91±0.09	7.1±2.6
	35±4	9.0±7.3	2.86±0.10	4.8±3.9
	59±3	11.6±3.5	2.88±0.06	6.4±1.9
TiO_2	7±1	7.0±1.4	1.09±0.12	10.1±2.0
	7±1	6.2±2.3	0.73±0.05	13.7±5.0
	33±3	17.9±5.6	2.23±0.03	12.7±3.9
	33±3	14.5±1.4	1.93±0.03	11.9±1.1

a: estimated upper limits.

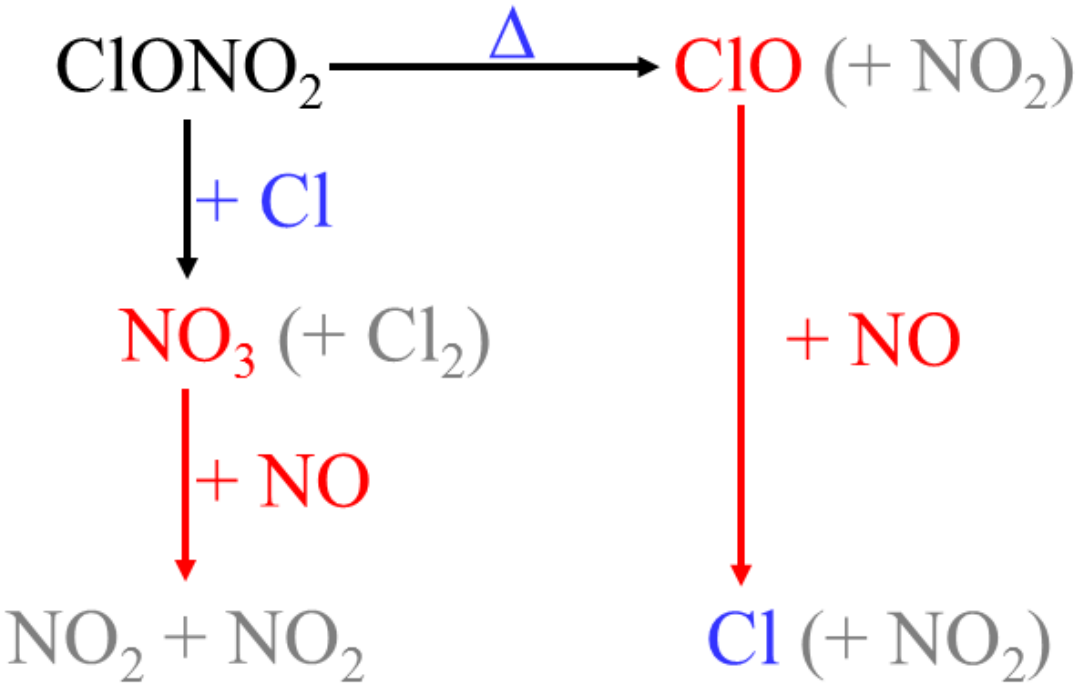

$$\text{Net: } [ClONO_2] = \Delta[NO]$$

935

936 **Scheme 1.** The $ClONO_2$ detection scheme used in our work.

937

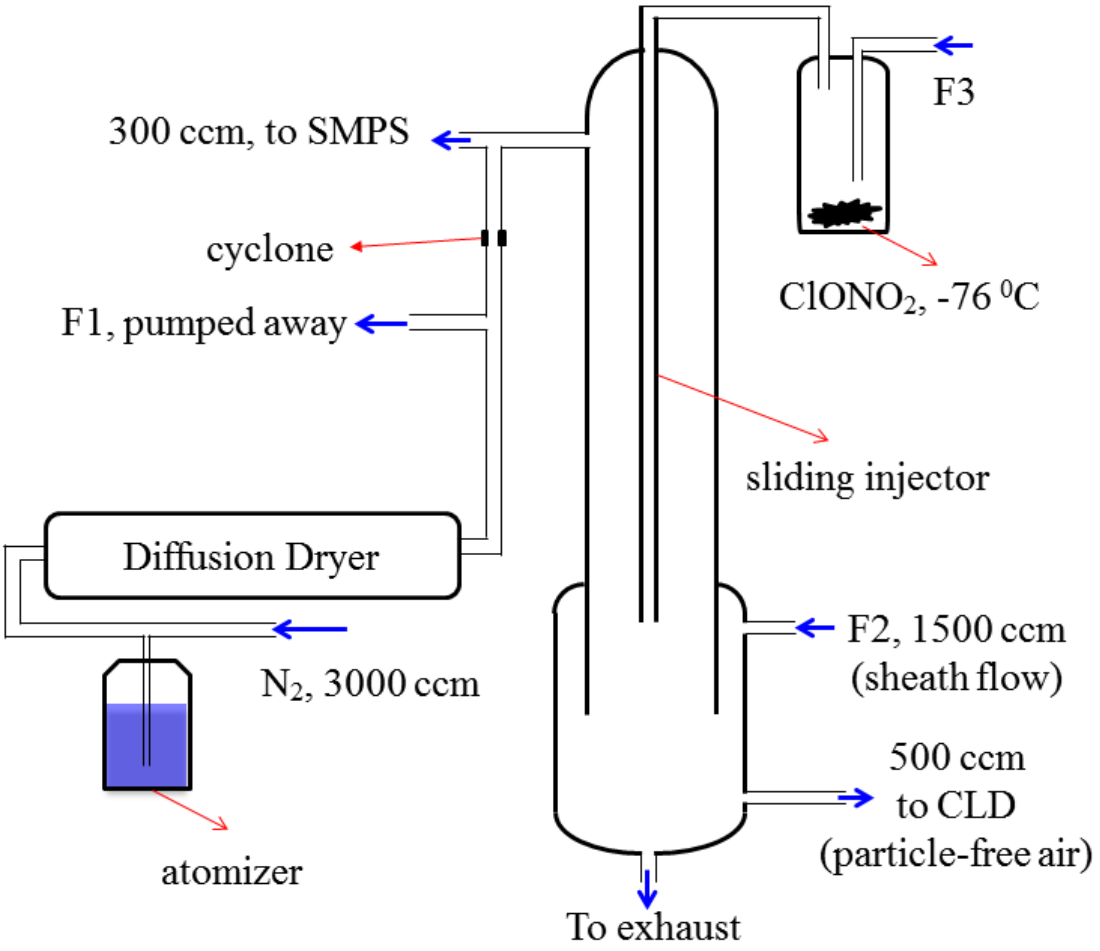

938

939 **Figure 1.** Schematic diagram of the aerosol flow tube used in this study. SMPS: Scanning
940 Mobility Particle Sizer; CLD: Chemiluminescence detector, used to measure the $ClONO_2$
941 concentration (measured as the change in NO concentration). All the flows (except the flow
942 applied to the atomizer) were controlled by mass flow controllers. Flow details are provided in
943 text.

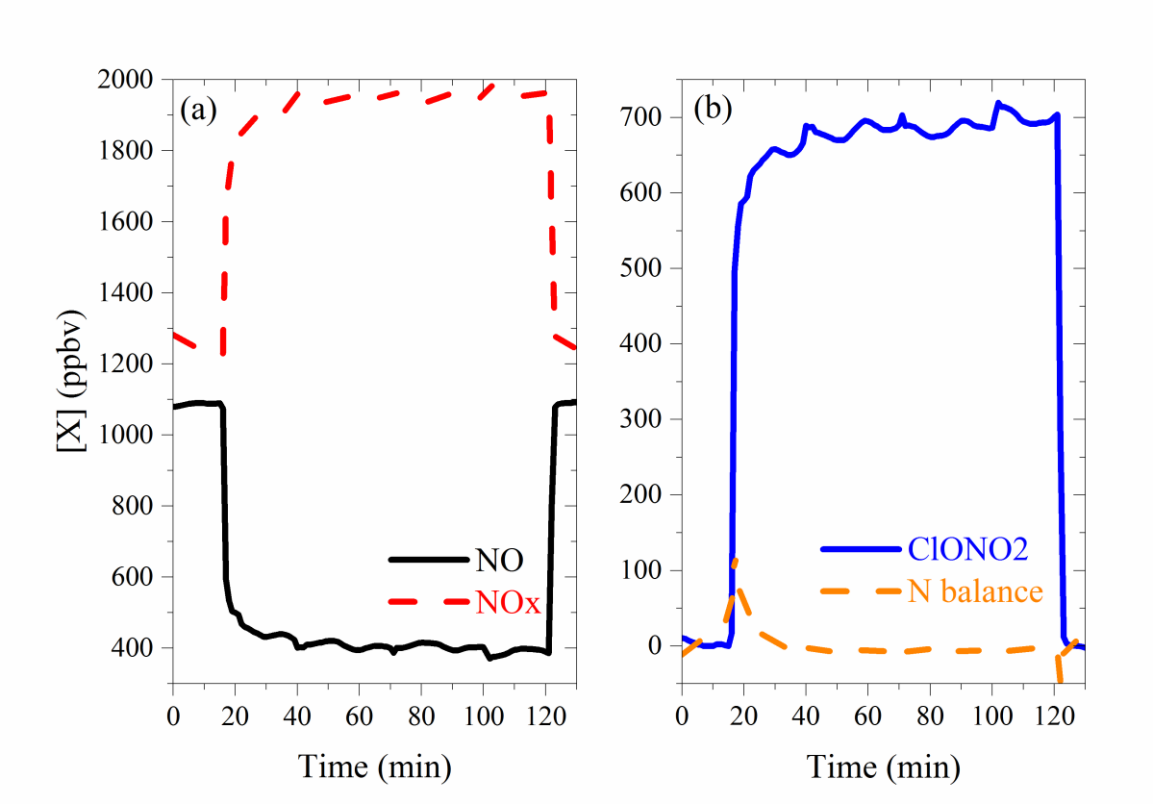

944

945 **Figure 2.** Response of measured NO and NOx mixing ratios to the introduction of $ClONO_2$

946 into the flow tube (left panel). The corresponding calculated $ClONO_2$ mixing ratio and nitrogen

947 balance are also shown (right panel).

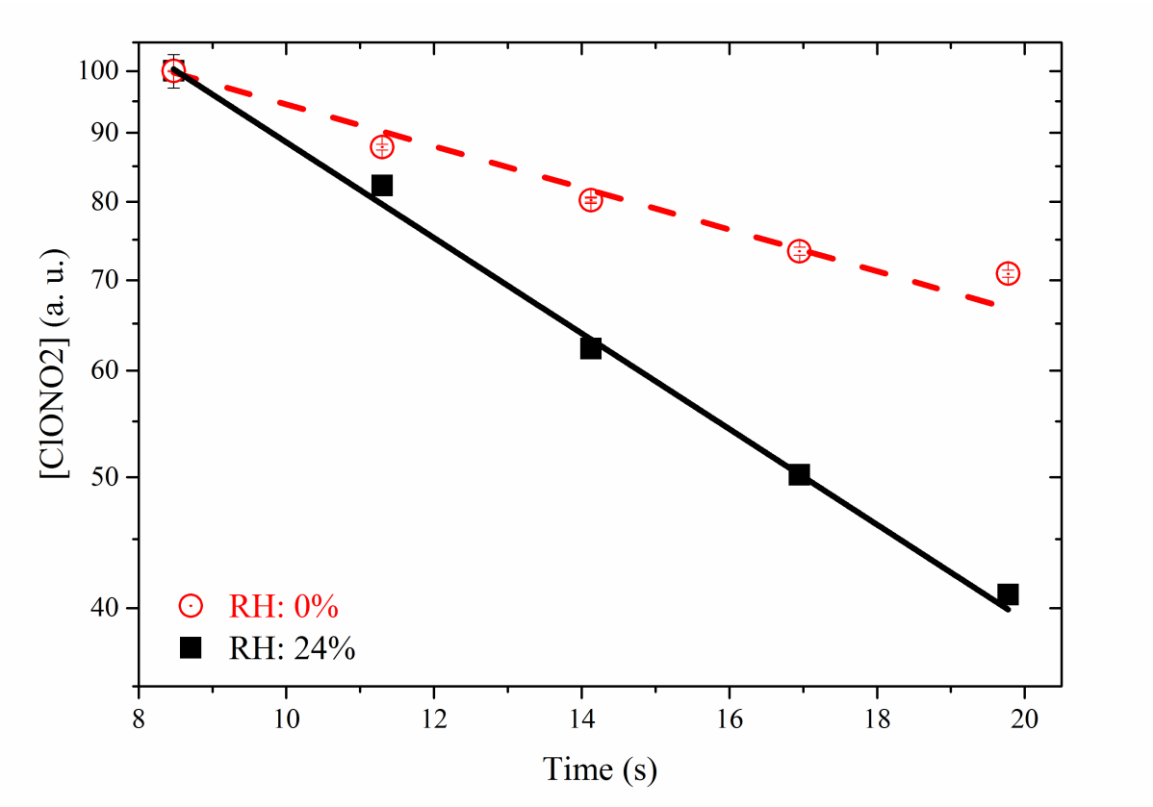

948

949 **Figure 3.** Decays of $ClONO_2$ in the flow tube due to its loss onto the Pyrex glass (circles: 0%
950 RH; squares: 24% RH). Measured $ClONO_2$ mixing ratios were normalized to that at 8.5 s (when
951 the injector was at 30 cm). Typical $ClONO_2$ mixing ratios in the flow tube are a few hundred
952 ppbv (see Figure 2).

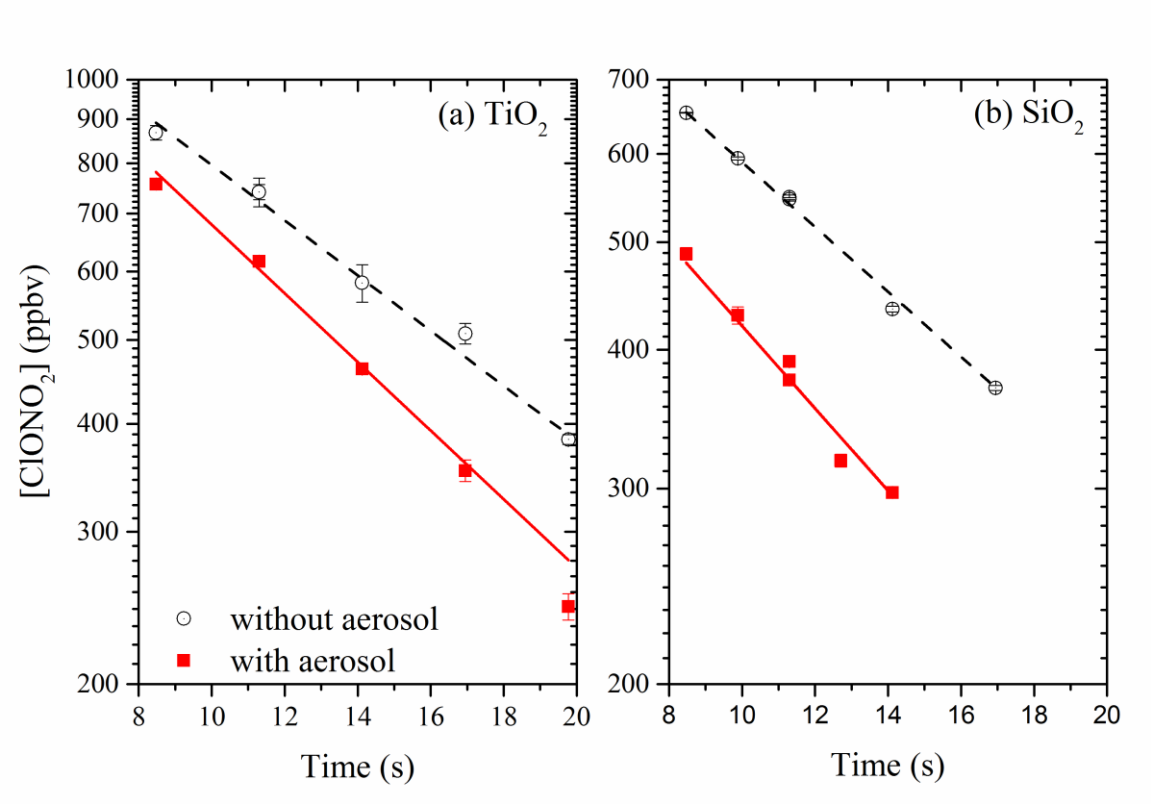

953

954 **Figure 4.** Decays of $ClONO_2$ in the aerosol flow tube without (open circles) and with (solid

955 squares) aerosol particles in the aerosol flow tube under different experimental conditions. (a)

956 TiO_2 with a surface area concentration of 2.3×10^{-3} cm^2 cm^{-3} at 33% RH; (b) SiO_2 with a surface

957 area concentration of 2.9×10^{-3} cm^2 cm^{-3} at 39% RH.

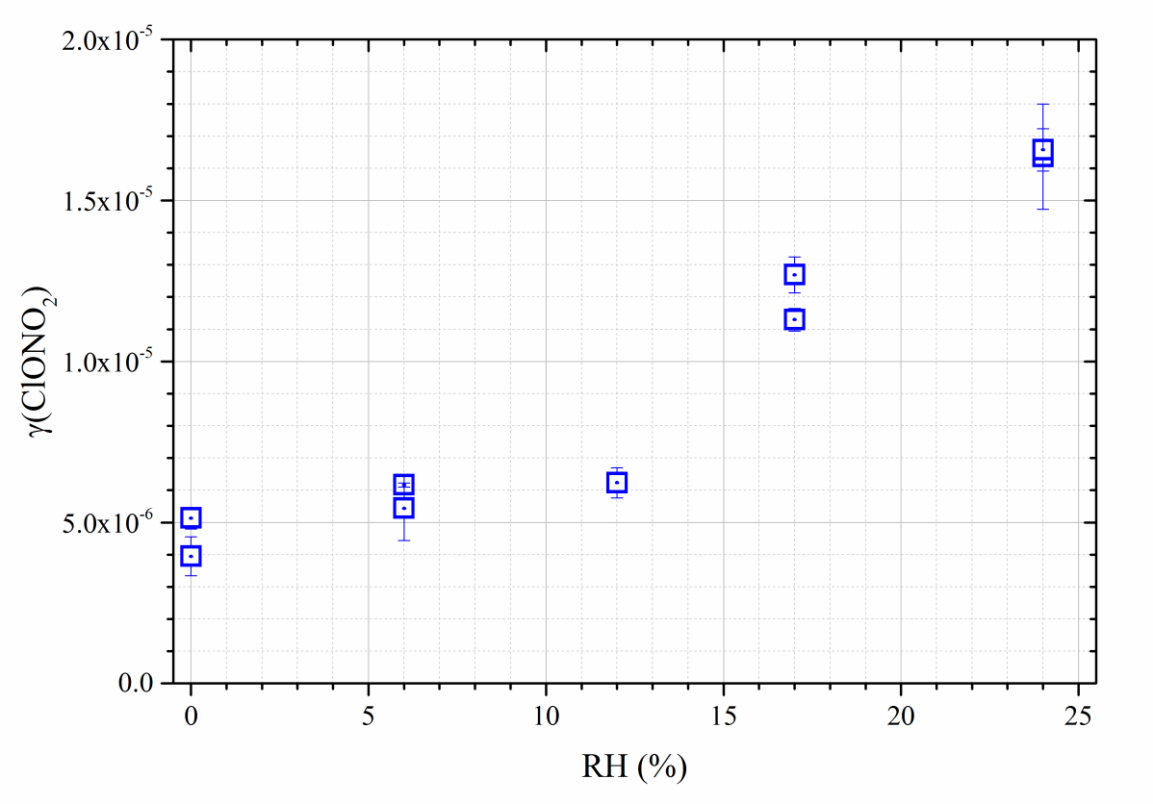

958

959 **Figure 5.** Dependence of $\gamma(ClONO_2)$ on RH for Pyrex glass.

960

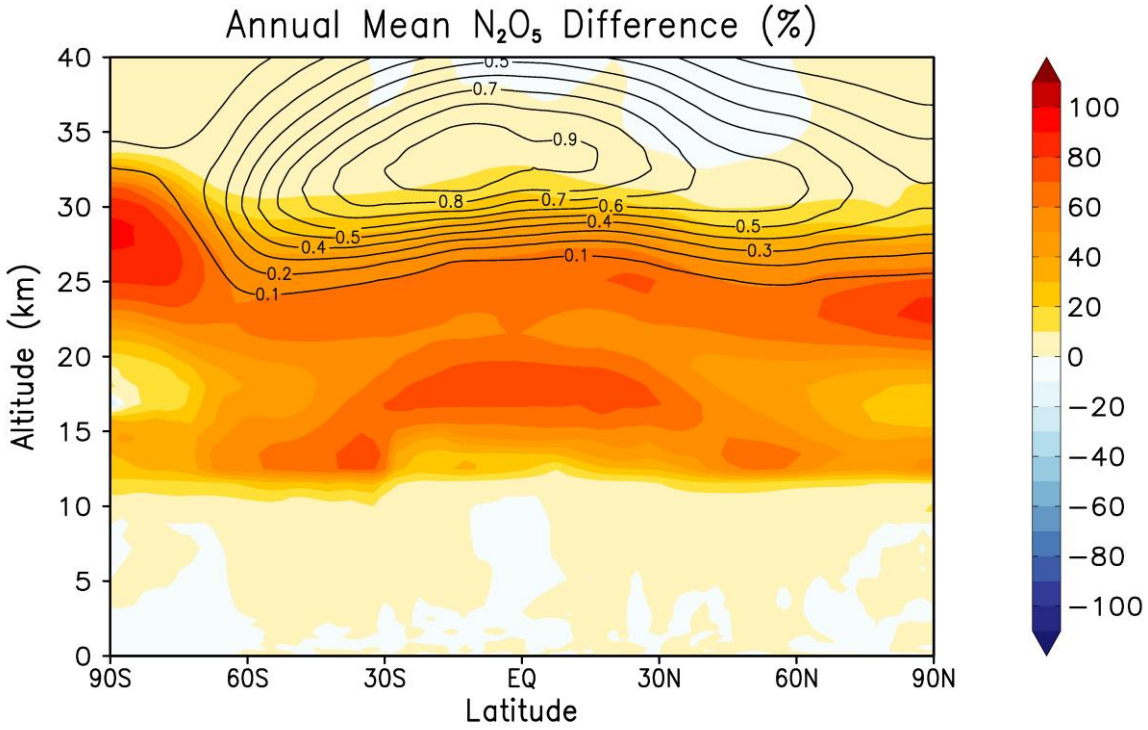

961
962 **Figure 6.** Simulated annual mean, zonal mean N_2O_5 percentage differences between TiO_2
963 injection (S3) and the Mt Pinatubo eruption (S2). Black contour lines show N_2O_5 mixing ratios
964 from the Mt Pinatubo simulation (S2) in ppb.

965

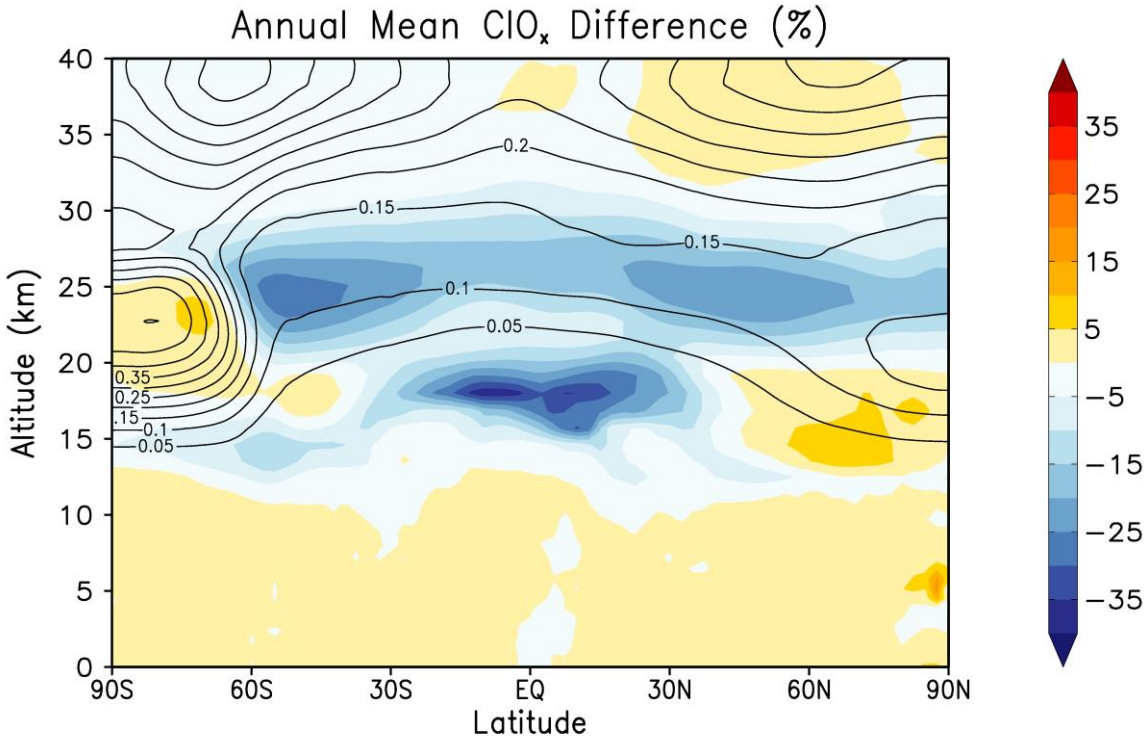

966

967 **Figure 7.** Simulated annual mean, zonal mean ClOx percentage differences between TiO_2

968 injection (S3) and the Mt Pinatubo eruption (S2). Black contour lines show ClOx mixing ratios

969 from the Mt Pinatubo simulation (S2) in ppb.

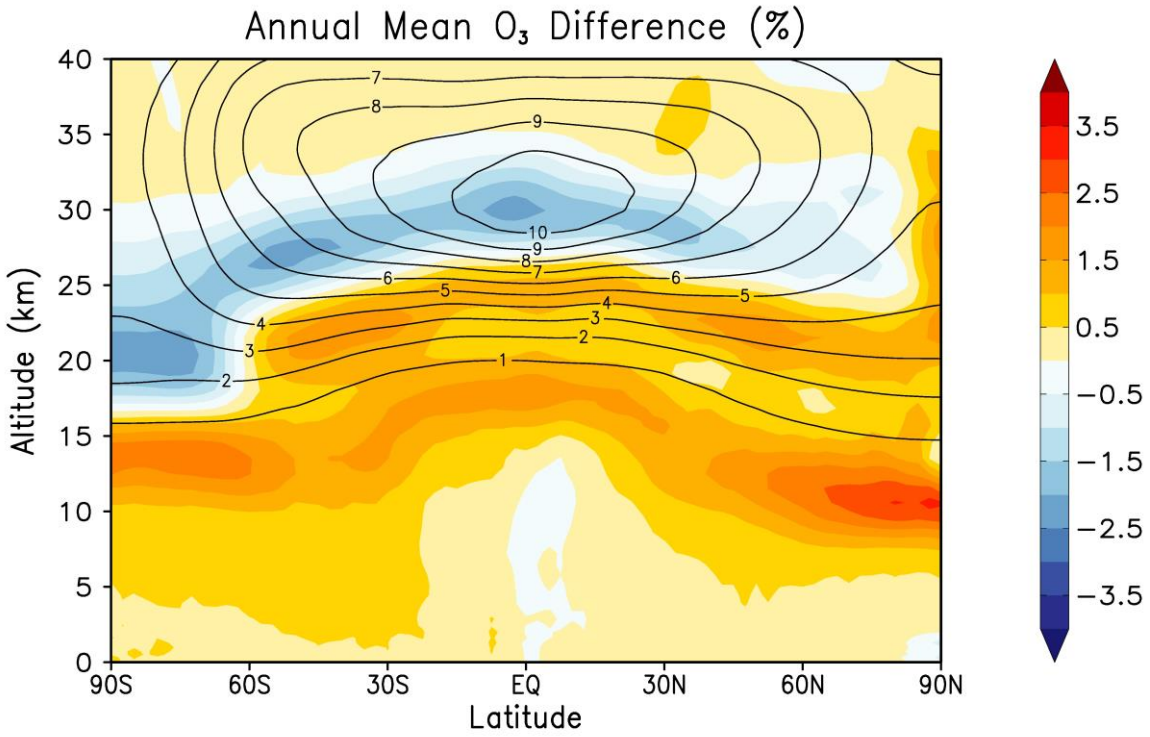

970

971 **Figure 8.** Simulated annual mean, zonal mean O_3 percentage differences between TiO_2

972 injection (S3) and the Mt Pinatubo eruption (S2). Black contour lines show ClOx mixing ratios

973 from the Mt Pinatubo simulation (S2) in ppmv.